The Preparation and Characterization of 4-Dimethylaminopyridine (DMAP) Stabilized Palladium Nanoparticles

Keith A. Flanagan, James A. Sullivan* and Helge Müeller Bunz.

UCD School of Chemistry and Chemical Biology, Belfield, Dublin 4, Ireland.

* Corresponding author

Abstract.

DMAP stabilized palladium nanoparticles with a mean diameter of 3.4 ± 0.5 nm are prepared from the aqueous phase reduction of Na_2PdCl_4 using $NaBH_4$ in the presence of DMAP. TEM and UV-Vis spectroscopy characterization of the nanoparticle dispersion shows no obvious change in the nanoparticles several months after preparation. ^{1}H NMR spectroscopy of the nanoparticles shows that the nanoparticle dispersion also contains a boron/DMAP complex and two palladium/DMAP complexes. One of the palladium complexes crystallizes out of the dispersion and is identified as $Pd(DMAP)_4(OH)_2$ by X-Ray Crystallography. Following extensive analysis it is believed that the palladium/DMAP complexes are formed following the oxidation of the palladium nanoparticles. The prepared nanoparticle dispersion promotes selective hydrogen/deuterium (H/D) exchange on the carbon atoms α to the endocyclic nitrogen atom on the DMAP stabilizing ligands through reaction with D_2O. This activity is attributed to the presence of the nanoparticles rather than to the presence of the oxidized palladium/DMAP complexes.

Keywords: Aqueous-phase palladium nanoparticles, DMAP stabilization, ^{1}H NMR spectroscopy characterization, aerobic oxidation and selective hydrogen/deuterium (H/D) exchange.

Introduction.

The ever-increasing interest in nanoparticles is attributed to the unique size dependent optical, electronic, magnetic and catalytic properties that they possess compared to both the corresponding bulk material and to the isolated atoms or molecules that make up the material.[1] The catalytic properties of metallic nanoparticles in particular have been extensively exploited in a variety of different chemical reactions.[2-6] The success observed using nanoparticles as catalysts has led to a growing demand for different types of nanoparticles which in turn has resulted in an exponential growth in the number of nanoparticle synthesis procedures reported.[2,4,5,7] However, despite the large number of preparation procedures reported there still exists a demand for new nanoparticle dispersions possessing nanoparticles with different sizes,[8,9] shapes [10,11] and stabilized by different types of ligands [12], which may possess distinctly different catalytic properties to other types of nanoparticle dispersions.

The choice of stabilizing ligand is extremely important when preparing transition metal nanoparticles and can have a dramatic effect on the catalytic properties of these nanoparticles. A balance is needed between the ability of a ligand to stabilize a nanoparticle while still allowing reactant molecules access to the nanoparticle surface for catalysis.[13] If bulky ligands are used, access to the nanoparticle surface for reactant molecules will be restricted due to steric crowding.[14,15] The use of DMAP as a stabilizing ligand for transition metal nanoparticles with potential catalytic properties is an intriguing prospect. Previously Gittins *et al.*[16] reported the synthesis of DMAP stabilized gold and palladium nanoparticles using a phase transfer procedure. Despite the extensive exploitation of the DMAP stabilized gold

nanoparticles in a number of various applications such as in the preparation of nanowires, [17] densely packed thin films [18,19] and light responsive microcapsules [20,21] DMAP stabilized palladium nanoparticles have not attracted as much interest with a notable exception being their use in catalytic microcapsules [22].

It is envisaged that palladium nanoparticles stabilized by DMAP could potentially be exploited more extensively in the field of catalysis. DMAP is an ideal ligand for stabilizing transition metal nanoparticles with catalytic properties due to the fact that it is not bulky, thereby allowing organic reactants access to the nanoparticle surface for catalysis. This is in contrast to the bulky stabilizers such as dendrimers, polymers and alkanethiols, which are typically used to sterically stabilize catalytic nanoparticles.[2,3] The fact that the use of DMAP as a stabilizing ligand results in aqueous phase nanoparticles could also be beneficial. Aqueous phase nanoparticles can potentially offer, economic, environmental and safety advantages over traditional organic solvent based catalysts and could lead to an increase in the use of water as a reaction medium and advance the area of green chemistry.[23,24] Furthermore, DMAP is versatile and can be easily removed by simple solvent washing or displaced by more strongly bound ligands. This could be exploited to immobilize nanoparticles onto suitable supports and thus form recyclable heterogeneous catalysts. This versatility could also be further exploited to prepare nanoparticles modified with a variety of interesting ligands via ligand-exchange processes,[25] for example nanoparticles modified with chiral ligands for use in asymmetric catalysis.

Before DMAP stabilized nanoparticles or indeed any other nanoparticles can be used as catalysts it is vital that they are fully characterized. A detailed pre-characterization

of the nanoparticle catalyst provides a distinct starting point from where the difficult task of determining the mechanism of nanoparticle catalysis in a particular synthetic reaction can begin *i.e.* in terms of identifying whether homogeneous or heterogeneous catalysis plays a role.[26,27] Identifying the exact mechanism by which nanoparticles catalyze different synthetic reactions is a necessary step in the development of more active and selective catalysts.

In this work we report an alternative facile one-phase synthesis method to prepare relatively monodisperse DMAP stabilized palladium nanoparticles. TEM and UV-Vis spectroscopy characterization of the nanoparticle dispersion shows no obvious change in the nanoparticles several months after preparation. ^{1}H NMR spectroscopy characterization on the other hand identifies the presence of several complexes in the dispersion namely two palladium/DMAP complexes and a boron/DMAP complex. The palladium/DMAP complexes are formed following oxidation of the palladium nanoparticles. This highlights the important role that ^{1}H NMR spectroscopy can play in characterizing nanoparticle dispersions and emphasizes the need for thorough characterization of nanoparticle dispersions prior to their use as catalysts.

^{1}H NMR spectroscopy also identifies the ability of the prepared nanoparticle dispersion to promote selective hydrogen/deuterium (H/D) exchange on the carbon atoms α to the endocyclic nitrogen atom on the DMAP stabilizing ligands through reaction with D_2O at room temperature and under atmospheric conditions. These DMAP stabilized palladium nanoparticles could potentially be further exploited as catalysts to selectively label other interesting molecules with deuterium for a variety of different applications.

Experimental Section.

Materials.

4-Dimethylaminopyridine, sodium borohydride, deuterium oxide 99.9 atom % D, 1-dodecanethiol, tetraoctylammonium bromide, chloroform, toluene, sodium hydroxide, sulfuric acid, anhydrous 1,4-dioxane, and anhydrous sodium sulfate were purchased from the Sigma-Aldrich Chemical Company Ltd. Potassium Bromide (Spectrosol) was purchased from BDH. Sodium tetrachloropalladate(II) was purchased from Reagecon. All chemicals were used as received without further purification. Multi-Walled-Carbon-Nanotubes (MWCNTs), prepared by a carbon arc discharge method, were supplied by the MER Corporation. Polycarbonate membrane filters (0.2 μm pore diameter) were purchased from Whatman-UK. The water used in all experiments was distilled deionized Millipore-MilliQ water (18 MΩ cm^{-1}).

A. Preparation of 4-Dimethylaminopyridine Stabilized Palladium Nanoparticles

Sodium tetrachloropalladate(II) (37.3 mg, 0.127 mmol) was dissolved in distilled-deionized water (3 mL) and stirred vigorously. 4-Dimethylaminopyridine (DMAP) (83.3 mg, 0.682 mmol) was sonicated into distilled-deionized water (9 mL) and added to the stirring solution of palladium salt. The resulting mixture was stirred for 20 minutes during which time a color change from an orange/yellow color to a clearer pale yellow color was observed.

The subsequent pale yellow solution was reduced by the addition of sodium borohydride (1 % w/v, 1.100 mL) in 0.100 mL aliquots. A color change from pale yellow to black was observed immediately. The resulting DMAP stabilized palladium

nanoparticles were stirred vigorously for a further 30 minutes and were fully characterized.

B. Preparation of 4-Dimethylaminopyridine Stabilized Palladium Nanoparticles in D_2O

DMAP stabilized palladium nanoparticles dispersed in D_2O were also prepared using the same procedure as described in Section (A) above except the quantities of reagents and volume of solvent used were scaled down to one third of the above preparation and D_2O was used instead of distilled-deionized water. The resulting DMAP stabilized palladium nanoparticles in D_2O were used for ^1H NMR spectroscopic characterization of the preparation.

C. Preparation of 4-Dimethylaminopyridine Stabilized Palladium Nanoparticles in D_2O and under Nitrogen

DMAP stabilized palladium nanoparticles were prepared under nitrogen in an effort to exclude oxygen. The quantities of reagents and volume of solvent used were scaled down to one third of the amounts stated in Section (A) above and D_2O was used instead of distilled-deionized water in the preparation as follows:

Sodium tetrachloropalladate(II) (12.4 mg, 0.042 mmol) in D_2O (2 mL) was heated to 100^oC for 30 minutes and subsequently bubbled with nitrogen for 30 minutes (Note: anhydrous 1,4-dioxane (4 μL, 46.941 μmol) was added as an internal standard at this point). Deaerated D_2O (2 mL), previously heated to 100^oC for 30 minutes and bubbled with nitrogen for 60 minutes was added to DMAP (27.8 mg, 0.228 mmol),

which had been dried on a schlenk line and the suspension was sonicated. The DMAP solution was added to the stirring solution of sodium tetrachloropalladate(II) and continuously bubbled with nitrogen. Deaerated D_2O (1 mL) was added to sodium borohydride (10.0 mg, 0.264 mmol), which had been dried on a schlenk line. The resulting 1 % w/v D_2O sodium borohydride solution (1 % w/v, 360 μL) was added dropwise to the deaerated solution of sodium tetrachloropalladate(II) and DMAP, which had been stirring for 20 minutes. The resulting black palladium nanoparticle dispersion was stirred vigorously for a further 30 minutes while bubbling nitrogen. The DMAP stabilized palladium nanoparticle dispersion was stored under nitrogen and samples extracted for ^{1}H NMR spectroscopic characterization. The extracted samples were injected into NMR tubes filled with nitrogen and sealed with a rubber septum. ^{1}H NMR spectra were obtained at various times after the nanoparticle dispersion preparation. Anhydrous 1,4-dioxane (resonance at δ 3.61) was used as an internal standard to monitor the concentration of palladium/DMAP complexes formed over time.

D. Removal of DMAP from the Palladium Nanoparticle Dispersion

DMAP stabilized palladium nanoparticles (2 mL) prepared as described in Section (A) were diluted to 10 mL with distilled-deionized water. The nanoparticles were successively washed with chloroform (10 mL) by vigorous mixing of the two layers until the nanoparticles had become destabilized and aggregated at the boundary between the water and chloroform layers. Typically 100mL of chloroform was sufficient to fully destabilize the nanoparticle dispersion indicating the successful removal of DMAP.

E. Phase Transfer of 4-Dimethylaminopyridine Stabilized Palladium Nanoparticles from an Aqueous Phase to an Organic Phase

DMAP stabilized palladium nanoparticles (2 mL) prepared as described in Section (A) were diluted to 10 mL with distilled-deionized water. Dodecanethiol (0.200 mL, 835 μmol) in 10 mL chloroform was added to the palladium nanoparticle dispersion and the resulting two-phase solution was stirred vigorously. Within 15 minutes, the organic phase began to turn brown, indicating phase transfer of the nanoparticles to the organic phase. The aqueous phase went clear following continued stirring for 10 hours indicating the complete phase transfer of the palladium nanoparticles to the organic phase. The resulting chloroform dispersion of palladium nanoparticles was characterized by TEM.

F. Preparation of 4-Dimethylaminopyridine Stabilized Palladium Nanoparticles Using a Phase Transfer Procedure

DMAP stabilized palladium nanoparticles were prepared using a phase transfer procedure reported by Gittins *et al.*[16] However, the quantities of reagents used were one-tenth of the amount stated and D_2O containing DMAP was used to facilitate phase transfer of the nanoparticles instead of water. The resulting dispersion of palladium nanoparticles in D_2O was characterized by TEM and ^1H NMR spectroscopic techniques.

G. Isolation of $Pd(DMAP)_4(OH)_2$ and Boron-DMAP complexes from the 4-Dimethylaminopyridine Stabilized Palladium Nanoparticle Dispersion

$Pd(DMAP)_4(OH)_2$ Complex

Crystals of $Pd(DMAP)_4(OH)_2$ formed following exposure of a DMAP stabilized palladium nanoparticle dispersion [prepared using the same procedure as described in Section (A)] to air for two weeks were removed from the nanoparticle dispersion by filtration. Further washing with small volumes of water (2-3 mL) removed any visible black nanoparticle residues remaining on the crystals. The isolated crystals, which were yellow in color, were dried on a schlenk line for 3 hours. These crystals were characterized using X-Ray crystallography, ^1H NMR spectroscopy and Mass spectrometry.

Boron-DMAP complex

Boron-DMAP complex was obtained from a DMAP stabilized palladium nanoparticle dispersion prepared using the same procedure as described in Section (A) above with the only difference being that 10 times more $NaBH_4$ was used.

Following addition of the reducing agent a large amount of white solid precipitate was observed immediately in the nanoparticle dispersion. Approximately one minute after the addition of reducing agent the resulting nanoparticle dispersion was removed from the reaction flask leaving behind the white solid on the flask walls. This procedure was repeated four times thus yielding four conical flasks covered with white solid (Boron-DMAP complexes). The resulting white solid was dissolved in water (10 mL) and any residual black nanoparticles were removed through their selective adsorption onto thiolated MWCNTs (4 mL). This suspension was then filtered through a

polycarbonate membrane filter (Whatman-UK, 0.2 μm pore diameter) to remove the MWCNT/nanoparticle composite, resulting in a clear solution. The solvent was then removed on a rotary evaporator and the resulting white solid was dried on a schlenk line for 2 hours. This solid was then characterized using ^{1}H NMR, ^{11}B NMR spectroscopy and Mass spectrometry.

Note: Thiolated Multi-Walled-Carbon-Nanotubes (MWCNTs) were prepared as reported.[52]

Measurement and Characterization Techniques

Transmission electron microscopy (TEM) images were recorded using a JEOL JEL-2000 EX electron microscope with a lattice resolution of 0.14 nm and a point-to-point resolution of 0.3 nm operating at 80 kV. All samples, unless stated otherwise, were prepared by evaporating a drop of the appropriate nanoparticle dispersion onto the surface of a carbon-coated 400 square mesh copper TEM grid.

UV-Visible absorption spectra were obtained on a Perkin Elmer Lambda 45 UV-Vis Spectrometer with UV WinLab software. All UV-Visible spectra were referenced using appropriate solution backgrounds.

Proton nuclear magnetic resonance spectra (^{1}H NMR) were recorded using a Varian 300 MHz FT-NMR spectrometer with either the solvent reference or TMS as the internal standard. All chemical shifts are quoted on the δ scale. All coupling constants are expressed in Hertz.

Boron nuclear magnetic resonance spectra (^{11}B NMR) were recorded using a Varian 400 MHz FT-NMR spectrometer.

X-Ray Crystallography was performed on a Bruker-AXS SMART Apex CCD three-circle diffractometer. A full sphere of the reciprocal space was scanned by phi-omega scans. Pseudo-empirical absorption correction based on redundant reflections was performed by the program SADABS.[28] The structure was solved by direct methods using SHELXS-97 [29] and refined by full matrix least-squares on F^2 for all data using SHELXL-97[30]. Hydrogen atoms attached to carbon were added at calculated positions and refined using a riding model. Their isotropic temperature factors were fixed to 1.2 times (1.5 times for methyl groups) the equivalent isotropic displacement parameters of the carbon atom the H-atom is attached to. Hydrogen atoms attached to oxygen could not be detected. The isotropic thermal displacement factors of the oxygen atoms of the partially occupied water molecules were constrained to be the equivalent isotropic displacement parameter of the $[OH]^-$ oxygen atom. Anisotropic temperature factors were used for all other atoms.

Electrospray Mass Spectrometry was performed on a Quattro Micro tandem quadrupole Mass Spectrometer (Waters Corporation, USA).

High resolution Mass Spectrometry was performed on a Liquid Chromatography time-of-flight (LCT) Mass Spectrometer (Waters Corporation, USA).

FTIR analysis was carried out within a Spectra Tech DRIFT cell using an ATI Mattson Infinity Series FTIR spectrophotometer equipped with a MCT detector.

Results and Discussion.

Initial Characterization of DMAP Stabilized Palladium Nanoparticles.

A representative TEM image of DMAP stabilized palladium nanoparticles prepared using the facile one-phase synthesis method described in the experimental section is shown in Figure 1.a. The nanoparticles possess an average diameter of 3.4 nm, and a standard deviation of ± 0.5 nm (calculated from the diameters of a sample of 330 nanoparticles (Figure 1.b). From a comparison of these palladium nanoparticles with those produced using the phase transfer procedure reported by Gittins *et al.*[16] (4.8 nm ± 1.2 nm) it is observed that smaller, more monodisperse (standard deviation: 14.7% compared to 25%) nanoparticles are obtained using the one-phase synthesis method. It is noted that when considering nanoparticles for use as catalysts that nanoparticle size can drastically affect catalytic activity.[31,32] Thus, monodisperse nanoparticle dispersions are preferred due to their more uniform catalytic properties in comparison to polydisperse nanoparticle dispersions.[33]

The prepared nanoparticles remain dispersed for several months with no obvious aggregation of the nanoparticles observed. TEM analysis of the nanoparticle dispersion several months after preparation confirmed that the nanoparticles still existed as individual entities. No discernible difference in the size or polydispersity of the nanoparticles was observed in comparison to a freshly prepared nanoparticle dispersion (Supporting Information, S1).

Figure 2 shows representative UV-Vis absorption spectra of the prepared DMAP stabilized palladium nanoparticle dispersion both 3 days, and 4 months after preparation. Both spectra feature a continual increase of absorbance at shorter wavelengths characteristic of nano-sized palladium, which can account for the overall black appearance of the dispersion.[34-36] Although both spectra show virtually identical profiles it is observed that there is a slight decrease in the overall absorbance observed for the 4 month old preparation in comparison to the 3-day-old preparation. This indicates that a certain proportion of the nanoparticles have been removed from the dispersion (see later). However, despite this, the virtually identical profiles of the 3-day-old and 4-month-old dispersions indicates that the nanoparticles remain dispersed for several months after preparation and this agrees with the TEM data above showing that the nanoparticles still exist as individual entities. Furthermore, there is no appearance of any absorbance band related to the formation of dissolved Pd species (see later).

In previous studies on DMAP stabilized gold nanoparticles it has been proposed that DMAP binds to the surface of gold nanoparticles in a perpendicular orientation via the lone pair of electrons on the endocyclic nitrogen atom.[16, 37-39] It is believed that electron delocalisation places a formal negative charge on the endocyclic nitrogen atom, which is highly favorable for bonding to the gold nanoparticle while concomitantly placing a formal positive charge on the exocyclic nitrogen atom. A similar weak non-covalent interaction would be expected for the DMAP stabilized palladium nanoparticles reported here (see Figure 3).

This weak non-covalent interaction between DMAP and the palladium nanoparticles was verified by the fact that successive chloroform washing was sufficient to remove the DMAP from the nanoparticle surface and cause the palladium nanoparticles to destabilize and aggregate. Ligands covalently bound to the nanoparticle surface cannot be removed by simple solvent washing.[16] The addition of chloroform containing dodecanethiol to the aqueous DMAP stabilized palladium nanoparticle dispersion followed by vigorous stirring results in the facile phase transfer of the palladium nanoparticles from the aqueous phase to the chloroform phase without drastically affecting the average nanoparticle diameter or polydispersity (Supporting Information, S2). This phase transfer of nanoparticles is due to the stronger binding affinity of thiols for the nanoparticle surface in comparison to DMAP. The hydrophobic dodecanethiol molecules displace DMAP from the surface of the nanoparticles at the boundary between the two phases. The dodecanethiol binds to the nanoparticle surface through the thiol sulfur while the alkane functionality of the ligand renders the overall nanoparticle surface hydrophobic and subsequently dispersible in the chloroform phase. The ease with which DMAP could be displaced by thiols further verified that the DMAP molecules are weakly physisorbed onto the palladium nanoparticle surface through a non-covalent interaction. Rucareanu *et al.* have recently reported similar ligand-exchange reactions involving DMAP stabilized gold nanoparticles and various different functionalized thiols.[25] As mentioned already the fact that DMAP can be easily displaced by more strongly bound ligands could be exploited to immobilize the palladium nanoparticles described here onto suitable supports thus forming recyclable heterogeneous catalysts. It may also be of benefit in terms of facilitating the access of reactants to the nanoparticle surface for catalysis.

^{1}H NMR Characterisation of the DMAP Stabilized Palladium Nanoparticle Dispersion.

TEM and UV-Vis spectroscopy characterization of the DMAP stabilized palladium nanoparticles prepared using the one-phase synthesis method has indicated that the nanoparticles remain dispersed for several months. ^{1}H NMR spectroscopy characterization of the nanoparticles prepared in D_2O highlighted a very important issue regarding the presence of DMAP complexes in the dispersion. To ensure that the D_2O preparation of the nanoparticles was otherwise identical to the aqueous preparation, the nanoparticles prepared in D_2O were firstly characterized by TEM. No measurable difference was observed between the nanoparticles obtained from the D_2O preparation and those obtained from the aqueous preparation (3.4 nm ± 0.5 nm) using TEM (Supporting Information, S3).

Figure 4 shows representative ^{1}H NMR spectra of (a) DMAP in D_2O and (b) the DMAP stabilized palladium nanoparticle dispersion in D_2O directly following preparation. The ^{1}H NMR spectrum of DMAP (Figure 4.a) displays resonances at δ 2.82, δ 6.49 and δ 7.91. These resonances are assigned to (1) the methyl group protons attached to the exocyclic nitrogen, (2) the symmetrical protons β to the endocyclic nitrogen and (3) the symmetrical protons α to the endocyclic nitrogen in the DMAP molecule, respectively. The resonance at δ 4.65 is due to water in the D_2O while it is also noted that small satellite resonances are quite often observed on either side of the main resonances due to the presence of naturally abundant ^{13}C isotope (~1%) in the molecule that splits the proton NMR signal.[40,41] In the ^{1}H NMR spectrum of the DMAP stabilized palladium nanoparticle dispersion in D_2O (Figure

4.b) resonances are observed at δ 2.88, δ 6.55 and δ 7.91 along with another set of smaller resonances at δ 3.04, δ 6.70 and δ 7.61. The position of the resonances at δ 2.88, δ 6.55 and δ 7.91 are virtually identical to the resonances displayed for DMAP in Figure 4.a and are thus attributed to the presence of the stabilizing DMAP ligand in the nanoparticle dispersion. These resonances are broader than the resonances observed in the ^{1}H NMR spectrum of just DMAP in the absence of the nanoparticles (see Figure 4.a).

Previous reports using NMR spectroscopy to characterize nanoparticles stabilized by pyridine and amines have attributed the broadening of resonances to a fast exchange process at the NMR timescale between excess free and bound ligands.[42-44] Excess DMAP is present in the nanoparticle dispersion and it is expected that DMAP molecules stabilize the palladium nanoparticles through a dynamic equilibrium between physisorbed and free DMAP. Therefore it is likely that the broadening of the DMAP resonances is also due to a fast exchange equilibrium between free and physisorbed DMAP. However, it must also be noted that other reports which described the characterization of nanoparticles stabilized by long alkane chain molecules using NMR spectroscopy attributed broadening to the high packing density of the alkane chain molecules along with spin–spin relaxation (T2) broadening and a distribution in the chemical shifts due to the different binding sites on the nanoparticle surface.[45-47] In any case such broadening is a recognized and accepted feature of resonances attributed to stabilizing ligands in nanoparticle dispersions.

The other set of smaller resonances observed in the DMAP stabilized palladium nanoparticle dispersion at δ 3.04, δ 6.70 and δ 7.61 is quite unexpected (Figure 4.b).

In general only one set of resonances is observed in the ^{1}H NMR spectrum of nanoparticles that can be attributed to stabilizing ligands on the nanoparticle surface or an excess of these ligands in the dispersion.[43-46] In a similar manner it is expected that only one set of resonances should be observed in the ^{1}H NMR spectrum of the DMAP stabilized palladium nanoparticle dispersion that can be attributed to DMAP physisorbed on the nanoparticles and free in solution.

Following multiple nanoparticle dispersion preparations and subsequent ^{1}H NMR spectroscopic characterization it was noted that three different extra resonance patterns could be observed in the nanoparticle dispersion spectra. These extra resonance patterns appeared close to those resonances attributed to DMAP in the nanoparticle dispersion. The three patterns observed were either at (a) δ 3.04, δ 6.70 and δ 7.61 (b) δ 2.77, δ 6.36 and δ 7.76 or (c) δ 2.91 and δ 7.84, see Supporting Information, S4 for representative ^{1}H NMR spectrum showing the resonance patterns (b) and (c). In some preparations the extra resonances appeared as a combination of two of these sets of resonances and sometimes all three sets of resonances were observed.

Griffin has previously observed the presence of additional resonances similar to those observed here in the ^{1}H NMR spectrum of a deliberately under-reduced preparation of DMAP stabilized gold nanoparticles.[38] Griffin concluded that the presence of these additional resonances was due to DMAP complexed to unreduced gold. The presence of multiple forms of DMAP complexed to gold resulted in the splitting of ^{1}H NMR resonances assigned to the DMAP molecule. These additional split resonances

appeared in the general region of the corresponding resonance for the equivalent proton in free DMAP. These extra resonances were not observed when the DMAP stabilized gold nanoparticles were fully reduced.

In a similar manner it is expected that the additional resonances observed in the DMAP stabilized palladium nanoparticle dispersion, which appear close to the resonances assigned to DMAP itself, are due to the presence of DMAP complexed with different species.

Characterization and Investigation into the Formation of DMAP Complexes.

In order to characterize the DMAP complexes present in the nanoparticle dispersion and understand their formation a systematic study of the preparation of the nanoparticle dispersion was carried out. Variables including the concentration of $NaBH_4$ used, the presence of an N_2 atmosphere, exposure to different amounts of air and the introduction of $NaBH_4$ reductant at different times during the preparation were altered during this study.

It was noted that in all DMAP stabilized palladium nanoparticle dispersion preparations a white precipitate was observed immediately after reduction of the sodium tetrachloropalladate(II)/DMAP precursor with $NaBH_4$, which then resolubilized with time. Increasing the amount of $NaBH_4$ used in the preparation increased the amount of white precipitate observed. This white solid was isolated from an over-reduced nanoparticle dispersion preparation as described in the

experimental section (section G) and then characterized using ^{1}H NMR and ^{11}B NMR spectroscopy along with Mass spectrometry (see Supporting Information S5).

The ^{1}H NMR spectrum of this white solid identified that this was the species that gave rise to the extra resonance pattern at (c) δ 2.91 and δ 7.84 seen in the nanoparticle dispersion. Mass spectrometry identified isotopic fragment patterns which conclusively indicated the presence of Boron within the species and specifically gave patterns that could be attributed to a Boron containing DMAP complex. The ^{11}B NMR spectrum also confirmed the presence of Boron in this DMAP complex. The resonance pattern attributed to this complex in the nanoparticle dispersion ^{1}H NMR spectrum disappears over time (presumably due to oxidation of the Boron-containing species with minute amounts of O_2 dissolved in the D_2O). This complex does not form in the absence of Pd, suggesting that Pd has some promoting role in its formation.

Preparation of the nanoparticle dispersion under a nitrogen atmosphere provided some extremely important information. Figure 5 shows the ^{1}H NMR spectrum of the dispersion immediately following a preparation under N_2. This shows that, apart from the resonances attributed to free and stabilizing DMAP, only resonance pattern (c) δ 2.91 and δ 7.84 attributed to Boron – DMAP complex is observed when the nanoparticles are prepared under a nitrogen atmosphere (note: resonance at δ 7.84 is observed as a shoulder on the resonance assigned to DMAP). Thus, under N_2 the DMAP complexes leading to the other two sets of resonance patterns (a) δ 3.04, δ 6.70 and δ 7.61 and (b) δ 2.77, δ 6.36 and δ 7.76 are not detectable.

However, over time a second DMAP complex (with ^{1}H NMR resonances at (a) δ 3.04, δ 6.70 and δ 7.61) was formed in the dispersion. These resonances increase over time (see Supporting Information Figure S6a) following an induction period of several hours and relate to a second of the three species formed in the original nanoparticle preparation (pattern a). Subsequent addition of $NaBH_4$ to a dispersion containing this complex removed these resonances (see Supporting Information Figure S6a). This indicates that this is an oxidized species, which probably forms through reaction with minute amounts of O_2 dissolved within the D_2O. It proved impossible to completely eradicate the formation of this species through degassing or nitrogen bubbling and efforts to isolate this complex also proved futile. However, we have shown that it is an oxidised species.

Exposure of a dispersion containing this complex to air resulted in two immediate effects (see Supporting Information S6b), *i.e.* a decrease in the resonances associated with the above mentioned reducible complex and an appearance of the final pattern of resonances seen in the original nanoparticle dispersion ((pattern b) δ 2.77, δ 6.36 and δ 7.76). This suggests that the former species can be converted into the latter upon exposure to air.

Leaving the dispersion exposed to air for 48 hours resulted in the formation of visible crystals. X-Ray crystallography identified the crystals present in the DMAP stabilized palladium nanoparticle dispersion as a $Pd(DMAP)_4(OH)_2$ square planar complex. As shown by the crystal structure obtained, (see Figure 6 and Supporting Information S7 for CIF file), the palladium ion is complexed to 4 DMAP ligands coordinated through their endocyclic nitrogen atoms giving a cationic species which is counter balanced by

two hydroxide (OH^-) anions. It is noted that the crystals were stored in the DMAP stabilized palladium nanoparticle aqueous dispersion (mother liquor) and only removed from the dispersion immediately prior to X-Ray crystallographic analysis. These crystals were isolated from the nanoparticle dispersion as outlined in the experimental section (Section G) and further Mass Spectrometry and ^1H NMR spectroscopy characterization of the isolated crystals was performed.

Mass Spectrometry of the isolated crystals gave a spectrum characteristic of the $Pd(DMAP)_4(OH)_2$ complex with a major peak at 297 a.m.u. within an isotopic pattern containing 7 peaks (consistent with the 6 isotopes of palladium).

The isolated crystals were found to be soluble in D_2O following sonication and vigorous stirring, subsequently a ^1H NMR spectrum of the isolated crystals could be obtained. Figure 7 shows a representative ^1H NMR spectrum of the $Pd(DMAP)_4(OH)_2$ complex crystals isolated from the DMAP stabilized palladium nanoparticle dispersion in D_2O.

The ^1H NMR spectrum of the isolated $Pd(DMAP)_4(OH)_2$ complex crystals displays two sets of resonances at (X) δ 2.85, δ 6.40 and δ 7.68 and (Y) δ 3.04, δ 6.72 and δ 7.85 ppm. The resonance set (Y) is attributed to trace amounts of free DMAP retained on the crystals following isolation from the nanoparticle dispersion. This was verified by gradual addition of extra DMAP to a D_2O solution of crystals, which resulted in an increase of the resonances in set (Y) in comparison to set (X) (Supporting

Information, S8.a). It is noted that the position of the resonances in the ^{1}H NMR spectrum of DMAP shift depending on the pH of the solution.

The remaining resonances in set (X) at δ 2.85, δ 6.40 and δ 7.68 are therefore attributed to the $Pd(DMAP)_4(OH)_2$ complex. These resonances are in similar positions to one set of the resonance patterns (pattern (b) δ 2.77, δ 6.36 and δ 7.76) noted from the one-phase DMAP stabilized palladium nanoparticle dispersion discussed above. Adjustment of the pH to that of the dispersion through the addition of DMAP results in the resonances of the $Pd(DMAP)_4(OH)_2$ complex moving to (δ 2.77, δ 6.37 and δ 7.79). This resonance pattern almost exactly matches those seen for the complex noted above ((pattern (b) δ 2.77, δ 6.36 and δ 7.76)) confirming that this isolated oxidised species is indeed the second oxidized species seen in the nanoparticle dispersion (see supporting information S8.b).

It is noted that $Pd(DMAP)_4(OH)_2$ complex crystals were consistently obtained from all nanoparticle dispersion preparations even those that originally did not show resonances directly attributed to this particular complex. Furthermore, ^{1}H NMR spectroscopy characterization of nanoparticle dispersions over several days identified that the resonances observed for the proposed palladium/DMAP complexes could interchange from one pattern to another over time under atmospheric conditions (Supporting Information, S9).

The addition of reducing agent (sodium borohydride) to a solution of the $Pd(DMAP)_4(OH)_2$ complex crystals resulted in an immediate color change and

yielded a black dispersion which indicated the reduction of the palladium(II) complex to palladium nanoparticles. TEM analysis of the black dispersion (see Figure 8.a) confirmed the presence of nanoparticles. The resulting nanoparticles possess an average diameter of 2.9 nm and a standard deviation of 0.7 nm (calculated from the diameters of a sample of 347 nanoparticles), see Figure 8.b. ^{1}H NMR spectroscopy characterization of a solution containing $Pd(DMAP)_4(OH)_2$ complex crystals with DMAP before and after addition of $NaBH_4$ confirmed the reduction of $Pd(DMAP)_4(OH)_2$ complex following addition of the reducing agent (see Figure 8.c).

The ease with which the $Pd(DMAP)_4(OH)_2$ complex (identified as one of the complexes present in the nanoparticle dispersion) can be reduced further clarifies the fact that this complex forms following oxidation of the nanoparticles rather than arising from interactions between unreduced precursor Pd(II) and DMAP.

This result and the plot shown in Supporting Information S6.a show that both of the Pd-containing complexes that appear in the dispersions prepared under N_2 (following (a) an induction period and (b) the introduction of air) can be removed through the addition of $NaBH_4$. This obviously suggests that they are reducible and thus products of oxidation.

Several factors make quantification of the concentration of these oxidized palladium/DMAP complexes in a typical palladium nanoparticle dispersion (*i.e.* prepared under atmospheric conditions) extremely difficult. These factors include (a) the transient nature of their formation, (b) the presence of two different resonance

patterns attributed to Pd-DMAP complexes, (c) the ability of resonance patterns to interchange over time, (d) the unknown nature of the first complex (pattern a) (in terms of the number of DMAP ligands) (e) the disappearance of resonances following the selective deuteration of DMAP (see later) and finally (f) the tendency of the second complex, $Pd(DMAP)_4(OH)_2$ to crystallize out of the nanoparticle dispersion over time.

However, despite these problems, an attempt was made to estimate the amount of DMAP present in the form of palladium/DMAP complexes within hours of the nanoparticle dispersion preparation using anhydrous 1,4-dioxane (resonance at δ 3.61) as an internal standard. This estimation suggested that roughly ~ 3% of the DMAP molecules were involved in Pd-complex formation and (given the relative proportions of DMAP and Pd in a typical preparation) this suggests that a short period of time following the formation of nanoparticles ~ 4% of the palladium in the dispersion is involved in complex formation (assuming each palladium ion binds four DMAP ligands as is the case in the $Pd(DMAP)_4(OH)_2$ complex).

It has been demonstrated that the DMAP stabilized palladium nanoparticles prepared using the one-phase synthesis method are readily oxidized resulting in the formation of palladium/DMAP complexes. In order to investigate whether this phenomenon is unique to the one-phase synthesis method described here, DMAP stabilized palladium nanoparticles have also been prepared using the phase-transfer procedure reported by Gittins *et al.*[16], see experimental section.

These nanoparticles were characterized by TEM and ^{1}H NMR spectroscopy. The nanoparticles were found to possess an average diameter of 5.4 nm ± 1.0 nm, which is similar to that originally reported by Gittins *et al.*[16] (Supporting Information, S10). Figure 9 shows the ^{1}H NMR spectrum of the phase-transferred DMAP stabilized palladium nanoparticles prepared in D_2O. The resonances observed at δ 2.19 and δ 7.14 are assigned to toluene present in the D_2O after phase transfer of the nanoparticles. The resonances observed at δ 2.86, δ 6.54 and δ 7.93 are again assigned to an equilibrium between DMAP physisorbed on the nanoparticle surface and free in solution. The additional resonances observed at δ 2.81, δ 6.39 and δ 7.71 are in similar positions to those previously attributed to $Pd(DMAP)_4(OH)_2$ complex in the DMAP stabilized palladium nanoparticle dispersion (pattern (b) discussed above) prepared using the one-phase synthesis method. This shows that palladium/DMAP complexes are also present in the nanoparticle dispersion prepared using this phase-transfer procedure. It also shows that the presence of complexes due to the oxidation of DMAP stabilized palladium nanoparticles is a general, previously undocumented, phenomenon relating to these aqueous phase nanoparticles.

Indeed the issue of palladium nanoparticle oxidation is a much wider issue in general that applies to various other nanoparticle preparation procedures. It has previously been shown that palladium nanoparticles stabilized by thiols,[48,49] polymers [50] and dendrimers [51] are also susceptible to oxidation. The oxidation of these nanoparticles was primarily identified using UV-Vis spectroscopy characterization with ^{1}H NMR spectroscopy also used by Shon *et al.*

The palladium/DMAP complexes formed following oxidation of the DMAP stabilized palladium nanoparticles, although clearly present in the dispersion (and identified by ^{1}H NMR spectroscopy), are not detectable using UV-Vis spectroscopy. Although a slight decrease in the overall UV-Vis absorbance is observed after several months no obvious absorption bands are observed that are attributable to these palladium/DMAP complexes (see UV-Vis Spectrum (S11) in Supporting Information). It is likely that the overall decrease in absorbance is attributed to the loss of a proportion of the nanoparticles presumably through a certain amount of oxidative dissolution and formation of palladium/DMAP complexes. In contrast to UV-Vis spectroscopy characterization these complexes are detectable using ^{1}H NMR spectroscopy thus highlighting the important role that ^{1}H NMR spectroscopy can play in characterizing nanoparticle dispersions and the detection of other dissolved species. Furthermore, the presence of these complexes can and actually does have a significant effect on the catalytic properties of the DMAP stabilized palladium nanoparticle dispersion, thus emphasizing the need for thorough characterization of nanoparticle dispersions before their use as catalysts or in any other application.[52]

Despite the presence of palladium/DMAP complexes following oxidation, the DMAP stabilized palladium nanoparticles remain dispersed for several months in contrast to some of the oxidized palladium nanoparticles discussed above [48,51]. The fact that the particles are initially susceptible to oxidation (with the formation of dissolved oxidized Pd(II) species) and yet are stable for periods of greater than 4 months seems to be an anomaly. Considering that the DMAP stabilized palladium nanoparticles are not fully dissolved into these ionic complexes over time suggests that the rate of the oxidation process decreases significantly after a relatively short period of time. It has

not been possible to measure the production of these oxidized species over extended periods of time due to the difficulties in quantification that have been discussed above. However, what is clear is that a large proportion of the nanoparticles remain dispersed and exist as individual entities for a significant period of time when they are simply stored in stoppered sample vials. Possible reasons for this "stability" can be postulated including the formation of DMAP overlayers [37] inhibiting successive oxidation or the formation of a passivating oxide surface layer on the nanoparticles themselves. It is noted that reactions where relatively old dispersions are used to catalyse selective deuteration through reactions with D_2O [57] (see later) proceed significantly more rapidly in the presence of H_2. This suggests that the nanoparticles exposed to air grow an oxide over-layer which can be removed through reaction with H_2.

The fact that the nanoparticles are not fully dissolved into palladium/DMAP complexes and do not aggregate over relatively long periods facilitates an assessment of the catalytic activity of the DMAP stabilized palladium nanoparticle dispersion and the influence of these complexes on the catalytic activity.[52]

Selective Hydrogen/Deuterium (H/D) Exchange on the Carbon Atoms α to the Endocyclic Nitrogen on DMAP in the Presence of Palladium Nanoparticles and D_2O.

Further analysis of the ^1H NMR spectra of DMAP stabilized palladium nanoparticles prepared in D_2O identified a very interesting issue. Figure 10 shows a comparison

between the ^{1}H NMR spectra of the DMAP stabilized palladium nanoparticle dispersion in D_2O obtained (a) one hour after preparation and (b) one day later.

It is observed that the resonances downfield in the ^{1}H NMR spectra of the nanoparticles at δ 7.91 and δ 7.61 attributed to DMAP and palladium/DMAP complexes, respectively begin to lesson and then virtually disappear after ~ 1 day in D_2O. These resonances downfield in the ^{1}H NMR spectrum of the DMAP stabilized palladium nanoparticle dispersion at ~ δ 8 are those that are attributed to the symmetrical protons α to the endocyclic nitrogen on DMAP.

As previously discussed it is expected that DMAP will bind to the palladium nanoparticles through this endocyclic nitrogen atom. [16, 37-39] A possible reason for the disappearance of the resonance at δ 7.91 assigned to DMAP could be the interaction of the ligand on the nanoparticle surface and broadening of the resonance into the baseline.[43-44,46,53-54] However, it should be noted that there is a large excess of DMAP in the dispersion so that at any given time it is expected that there should be a significant amount of DMAP molecules not coordinated to the palladium nanoparticles. Furthermore, this does not explain why the resonance at δ 7.61 attributed to DMAP in the aforementioned palladium/DMAP complexes would also disappear.

It is noted that the resonances for the symmetrical protons α to the endocyclic nitrogen atoms on virtually all the DMAP molecules (equilibrated between free and physisorbed on the nanoparticle surface as well as present in the form of palladium/DMAP complexes) have disappeared while those attributed to the

symmetrical protons β to the endocyclic nitrogen and the methyl group protons attached to the exocyclic nitrogen remain unaffected. Considering this it is suggested that selective hydrogen/deuterium (H/D) exchange occurs on the carbons α to the endocyclic nitrogen atom on DMAP through reaction with D_2O and catalyzed by the palladium nanoparticle dispersion.

In order to verify this hypothesis, DMAP was removed from a DMAP stabilized palladium nanoparticle dispersion prepared in D_2O after 1 day by successive washing with chloroform as outlined in the experimental section. This DMAP was compared to as-received DMAP (99% pure) using FTIR spectroscopy and High-Resolution Mass Spectrometry. FTIR spectroscopy (Supporting Information, S11) shows that the aromatic C-H stretches at 3035 and 2295 cm^{-1} observed for DMAP (99% pure) are not observed for the DMAP removed from the nanoparticle dispersion prepared in D_2O and that a peak at 2235 cm^{-1} is observed instead. This indicated replacement of hydrogen with deuterium in the aromatic ring.[55, 56] The C-H out of plane bend (at 810 cm^{-1}) was also removed upon deuteration and several extra peaks were introduced in this region. High-Resolution Mass Spectrometry also clearly shows that the molecular mass of DMAP increased by ~2 a.m.u. when present in the nanoparticle dispersion prepared in D_2O. This data confirmed that selective hydrogen/deuterium (H/D) exchange had occurred on the carbons α to the endocyclic nitrogen atom on DMAP at room temperature and under atmospheric conditions.

Separate experiments where $Pd(DMAP)_4(OH)_2$ complex crystals are isolated from a water-based dispersion and subsequently dissolved in D_2O along with additional DMAP, show no disappearance in the resonances of the symmetrical protons α to the

endocyclic nitrogen atoms *i.e.* there is no selective hydrogen/deuterium (H/D) exchange on the carbons α to the endocyclic nitrogen atom on DMAP under these conditions (Supporting Information, S13). This suggests that the palladium nanoparticles play an intimate part in the deuteration process activating the DMAP towards base catalyzed hydrogen exchange reactions, presumably by stabilizing a negative charge on a de-protonated carbon α to the endocyclic nitrogen atom.

The ability to selectively label molecules with deuterium is extremely important in pharmacological, chemical and environmental research areas especially for the investigation of reaction mechanisms and kinetics.[57-59] Deuterated molecules can be used in stable isotopic tracer studies where they can be detected using mass spectrometry. Furthermore, deuterium labeling provides a route to obtain tritium labeled molecules for radiotracer studies.[60] It is envisaged that the DMAP stabilized palladium nanoparticles described here could potentially be further exploited as convenient, safe and economical catalysts in the selective deuterium labeling of other interesting molecules for a variety of different applications. [52]

The fact that the carbon atoms α to the endocyclic nitrogen atom on DMAP undergo selective hydrogen/deuterium (H/D) exchange rather than the carbon atoms β to the endocyclic nitrogen and the methyl group carbons attached to the exocyclic nitrogen also appears to further verify that DMAP binds to the palladium nanoparticles through the endocyclic nitrogen as has been postulated previously by other researchers for DMAP stabilized metallic nanoparticles.[16, 37-39]

Conclusions.

The facile aqueous-phase synthesis of relatively monodisperse DMAP stabilized palladium nanoparticles has been reported. The presence of DMAP complexes within the dispersion including a Boron-DMAP complex and two oxidized palladium/DMAP complexes has been identified as a general feature of this aqueous phase DMAP stabilized palladium nanoparticle dispersion. Oxidised Pd complexes are formed by the oxidation of palladium(0) nanoparticles and are present in all DMAP stabilized palladium nanoparticle dispersions whether produced via a one-phase synthesis method as described here or via a previously established phase-transfer procedure. ^{1}H NMR spectroscopy has been used to identify these two palladium complexes in the one-phase synthesis nanoparticle dispersion and one of these complexes has been isolated and definitively characterized by X-Ray crystallography as $Pd(DMAP)_4(OH)_2$. The presence of these oxidized species has little measurable impact on the stability of the remainder of the nanoparticles for periods of more than 4 months.

The one-phase synthesis nanoparticle dispersion promotes selective (H/D) hydrogen/deuterium exchange on the carbon atoms α to the endocyclic nitrogen atom on the DMAP stabilizing ligands in the presence of D_2O and this activity is attributed to the nanoparticles rather than to the above-mentioned complexes.

Acknowledgements:

We would like to acknowledge fruitful discussions with Prof. M. Brust and Prof. R. More O'Ferrall along with advice from Prof D Fitzmaurice. We gratefully thank Dr. Dilip Rai for all mass spectrometry analysis.

Supporting Information Available:

S1. TEM image of DMAP stabilized palladium nanoparticles 4 months after preparation.

S2. TEM image of phase-transferred dodecanethiol stabilized palladium nanoparticles.

S3. TEM image of DMAP stabilized palladium nanoparticles prepared in D_2O.

S4. ^{1}H NMR spectrum of the DMAP stabilized palladium nanoparticle dispersion in D_2O showing the extra resonance patterns at (b) and (c) attributed to DMAP complexes.

S5. ^{1}H NMR and ^{11}B NMR spectra along with Mass spectrum of the Boron/DMAP complex.

S6. Plots of the concentration of the Pd-DMAP complexes present in a nanoparticle dispersion prepared under nitrogen as a function of time, addition of $NaBH_4$ and exposure to air.

S7. CIF File data relating to the crystal structure determination of the isolated $Pd(DMAP)_4(OH)_2$ complex.

S8. ^{1}H NMR spectra of isolated $Pd(DMAP)_4(OH)_2$ complex crystals with an increasing amount of added DMAP and an additional spectrum showing the movement of the resonances attributed to $Pd(DMAP)_4(OH)_2$ complex to pattern (b) seen in the nanoparticle dispersion upon increasing the pH.

S9. ^{1}H NMR spectra of the DMAP stabilized palladium nanoparticle dispersion in D_2O obtained (a) one hour and (b) five days after preparation demonstrating that the resonances observed for palladium/DMAP complexes could interchange from one pattern to another over time.

S10. TEM image of DMAP stabilized palladium nanoparticles prepared using the phase-transfer procedure reported by Gittins *et al.*[16] in D_2O.

S11. UV-Vis absorption spectra of DMAP stabilized palladium nanoparticles 3 days and 4 months after preparation along with a spectrum of a solution of $Pd(DMAP)_4(OH)_2$ crystals.

S12. FTIR spectra of 99% pure DMAP and deuterated DMAP following selective hydrogen/deuterium (H/D) exchange.

S13. ^1H NMR spectrum of $Pd(DMAP)_4(OH)_2$ complex and additional DMAP showing no selective hydrogen/deuterium (H/D) exchange on the carbon atoms α to the endocyclic nitrogen atom on DMAP in the absence of nanoparticles.

This material is available free of charge via http://pubs.acs.org.

References:

(1) Zhang, J.Z.; Wang, Z-l.; Liu, J.; Chen, S.; Liu, G-y *Self Assembled Nanostructures*, Kluwer Academic/Plenum Publishers, 2002.

(2) Astruc, D.; *Inorg. Chem.* **2007**, *46*, 1884.

(3) Astruc, D.; Lu, F.; Aranzaes, J.R. *Angew. Chem. Int. Ed.* **2005**, *44*, 7852.

(4) Roucoux, A.; Schulz, J.; Patin, H. *Chem. Rev.* **2002**, *102*, 3757.

(5) Aiken (III) J.D.; Finke, R.G. *J. Mol. Catal. A: Chem.* **1999**, *145*, 1.

(6) Moreno-Manas M.; Pleixats R. *Acc. Chem. Res.* **2003**, *36*, 638.

(7) Bonnemann, H.; Richards, R.M. *Eur. J. Inorg. Chem.* **2001**, *10*, 2455.

(8) Li, Y.; Boone, E.; El-Sayed, M. A. *Langmuir,* **2002**, *18*, 4921.

(9) Wilson, O. M.; Knecht, M. R.; Garcia-Martinez, J. C.; Crooks, R. M. *J. Am. Chem. Soc.* **2006**, *128,* 4510.

(10) Narayanan, R.; El-Sayed, M. A. *Nano Lett.* **2004**, *4*, 1343.

(11) Narayanan, R.; El-Sayed, M. A. *J. Phys. Chem. B.* **2005**, *109*, 12663.

(12) Tamura, M.; Fujihara, H.; *J. Am. Chem. Soc.* **2003**, *125*, 15742.

(13) Klabunde, K.J. *Nanoscale Materials in Chemistry*, Wiley-Interscience, 2001.

(14) Oh, S-K.; Niu, Y.; Crooks, R. M. *Langmuir*, **2005**, *21,* 10209.

(15) Zhao, M.; Crooks, R. M. *Angew. Chem. Int. Ed.* **1999**, *38*, 364.

(16) Gittins, D.I.; Caruso, F. *Angew. Chem. Int. Ed.* **2001**, *40*, 3001.

(17) Ongaro, A.; Griffin, F.; Beecher, P.; Nagle, L.; Iacopino, D.; Quinn, A.; Redmond, G.; Fitzmaurice, D. *Chem. Mater.* **2005,** *17*, 1959.

(18) Yu, A.; Liang, Z.; Cho, J.; Caruso, F. *Nano. Lett.* **2003**, *3*, 1203.

(19) Cho, J.; Jang, H.; Yeom, B.; Kim, H.; Kim, R.; Kim, S.; Char, K.; Caruso, F *Langmuir*, **2006,** *22,* 1356.

(20) Angelatos, A. S.; Radt, B.; Caruso, F. *J. Phys. Chem. B*. **2005,** *109,* 3071.

(21) Radt, B.; Smith, T.A.; Caruso, F. *Adv. Mater.* **2004**, *16*, 2184.

(22) Turkenburg, D.H.; Antipov, A.A.; Thathager, M.B.; Rothenberg, G.; Sukhorukov, G.B.; Eiser, E. *Phys. Chem. Chem. Phys.* **2005**, *7*, 2237.

(23) Shaughnessy, K.H.; DeVasher, R.B. *Curr. Org. Chem.* **2005**, *9*, 585.

(24) Vasylyev, M.V.; Maayan, G.; Hovav, Y.; Haimov, A.; Neumann, R. *Org. Lett.* **2006**, *8*, 5445.

(25) Rucareanu, S.; Gandubert V.J.; Lennox R.B. *Chem. Mater.* **2006**, *18*, 4674.

(26) Phan, N.T.S.; Van Der Sluys, M.; Jones, C.W. *Adv. Synth. Catal.* **2006**, *348*, 609.

(27) Widegren, J.A.; Finke, R.G. *J. Mol. Catal. A: Chem.* **2003**, *198*, 317.

(28) Sheldrick, G.M. SADABS, Bruker AXS Inc., Madison, WI 53711, 2000.

(29) Sheldrick, G. M., SHELXS-97, University of Göttingen 1997.

(30) Sheldrick, G. M., SHELXL-97-2, University of Göttingen 1997.

(31) Roduner, E. *Chem. Soc. Rev.* **2006**, *35*, 583.

(32) Roduner, E. *Nanoscopic Materials: Size-Dependent Phenomena*, RSC Publishing, 2006.

(33) Sugimoto, T. *Monodispersed Particles*, Elsevier, 2001.

(34) Creighton, J.A.; Eadon, D.G. *J. Chem. Soc., Faraday Trans.* **1991**, *87*, 3881.

(35) Henglein, A. *J. Phys. Chem. B.* **2000**, *104,* 6683.

(36) Chen, M.; Falkner, J.; Guo, W-H.; Zhang, J-Y.; Sayes, C. ; Colvin, V.L. *J. Colloid Interface Sci.* **2005**, *287*, 146.

(37) Gandubert V.J.; Lennox R.B. *Langmuir*, **2005**, *21,* 6532.

(38) Griffin, F.; Fitzmaurice, D. *Langmuir,* **ASAP Article 2007** DOI:10.1021/la061261a S0743-7463(06)01261-3.

(39) Barlow, B.C.; Burgess, I.J.; *Langmuir*, **2007**, *23*, 1555.

(40) Cohen, A.D.; Sheppard, N.; Turner, J.J. *J. Proc. Chem. Soc.* **1958**, 118.

(41) Brownstein, S. *Chem. Rev.* **1959**, *59,* 463.

(42) Hens, Z.; Moreels, I.; Martins, J.C. *ChemPhysChem*, **2005**, *6*, 2578.

(43) Ramirez, E.; Jansat, S.; Philippot, K.; Lecante, P.; Gomez, M.; Masdeu-Bulto, A.M.; Chaudret, B. *J. Organomet. Chem.* **2004**, *689*, 4601.

(44) Pan, C.; Pelzer, K.; Philippot, K.; Chaudret, B.; Dassenoy, P.L.; Casanove, M-J. *J. Am. Chem. Soc.* **2001***, 123,* 7584.

(45) Hostetler, M.L.; Wingate, J.E.; Zhong, C-J.; Harris, J.E.; Vachet, R.W.; Clark, M.R.; Londono, J.D.; Green, S.J.; Stokes, J.J.; Wignall, G.D.; Glish, G.L.; Porter, M.D.; Evans, N.D.; Murray, R.D. *Langmuir*, **1998**, *14*, 17.

(46) Badia, A.; Singh, S.; Demers, L.; Cuccia, L.; Brown, G.; Lennox, R.B. *Chem. Eur. J.* **1996**, *2*, 359.

(47) Zamborini, F.P.; Gross, S.M.; Murray, R.W. *Langmuir*, **2001**, *17*, 481.

(48) Chen, M.; Feng, L-y.; Zhang, L.; Zhang, J-Y. *Colloids Surf., A*. **2006**, *281*, 119.

(49) Shon, Y-S.; Cutler, E. *Langmuir*, **2004**, *20*, 6626.

(50) Xiong, Y.; Chen, J.; Wiley, B.; Xia, Y.; Aloni, S.; Yin, Y. *J. Am. Chem. Soc.* **2005**, *127*, 7332.

(51) Scott R.W.J.; Ye H.; Henriquez R.R.; Crooks R.M. *Chem. Mater.* **2003**, *15*, 3873.

(52) Flanagan, K.A., Ph.D. Thesis, UCD, April 2007.

(53) Terrill, R.; Postlethwaite, T.; Chen, C.; Poon, C.; Terzis, A.; Chen, A.; Hutchison, J.; Clark, R.; Wignall, G.; Londono, J.; Superfine, R.; Falvo, M.; Johnson, C.; Samulski, E.; Murray, R. *J. Am. Chem. Soc.* **1995***, 117,* 12537.

(54) Naka, K.; Yaguchi, M.; Chujo, Y. *Chem. Mater.* **1999**, *11*, 849.

(55) Peeters, E.; Allamandola, L.J.; Bauschlicher Jr., C.W.; Hudgins, D.M.; Sandford, S.A.; Tielens, A.G.G.M. *ApJ* **2004**, *604*, 252.

(56) Bauschlicher Jr., C.W.; Langhoff, S.R.; Sandford, S.A.; Hudgins, D.M. *J. Phys. Chem. A*, **1997**, *101*, 2414.

(57) Derdau, V.; Atzrodt, J. *SynLett*. **2006**, *12*, 1918.

(58) Junk, T.; Catallo, W.J. *Chem. Soc. Rev.* **1997**, *26*, 401.

(59) Ito, N.; Watahiki, T.; Maesawa, T.; Maegawa, T.; Sajiki, H. *Adv. Synth. Catal.* **2006**, *348*, 1025.

(60) Alexakis, E.; Jones, J.R.; Lockley, W.J.S. *Tetrahedron Lett.* **2006**, *47*, 5025.

Figure Captions

Figure 1: (a) Transmission electron micrograph of the DMAP stabilized palladium nanoparticles. (b) Histogram of the diameters of 330 nanoparticles with an average diameter of 3.4 nm and a standard deviation of ± 0.5 nm.

Figure 2: UV-Vis absorption spectra of DMAP stabilized palladium nanoparticles 3 days and 4 months after preparation (The dispersion was diluted 1 in 25 with water).

Figure 3: The resonance structures of the DMAP molecule and its proposed interaction with the surface of a palladium nanoparticle.

Figure 4: Representative ^{1}H NMR spectra of (a) DMAP in D_2O and (b) the DMAP stabilized palladium nanoparticle dispersion in D_2O directly following preparation.

Figure 5: (a) ^{1}H NMR spectrum of the DMAP stabilized palladium nanoparticle dispersion prepared under an N_2 atmosphere (Resonance at δ 3.61 is attributed to anhydrous 1,4-dioxane, which is used as an internal standard). (b) Magnification of spectrum showing the absence of the other two sets of resonance patterns (a) δ 3.04, δ 6.70 and δ 7.61 and (b) δ 2.77, δ 6.36 and δ 7.76.

Figure 6: X-Ray crystal structure of the crystals isolated from the DMAP stabilized palladium nanoparticle dispersion: (a) The cationic complex with the two closest counterions and (b) View along [0 1 0]; the thermal ellipsoids are drawn on the 15% probability level.

Figure 7: ^{1}H NMR spectrum of the crystals isolated from the DMAP stabilized palladium nanoparticle dispersion.

Figure 8: (a) Transmission electron micrograph of the palladium nanoparticles obtained after reduction of a solution of $Pd(DMAP)_4(OH)_2$ complex crystals. (b) Histogram of the diameters of 347 nanoparticles with an average diameter of 2.9 nm and a standard deviation of ± 0.7 nm. (c) ^{1}H NMR spectrum of Pd $Pd(DMAP)_4(OH)_2$ complex and DMAP before and after addition of $NaBH_4$. The resonances attributed to $Pd(DMAP)_4(OH)_2$ complex are decreased significantly indicating reduction of the complex.

Figure 9: ^{1}H NMR spectrum of phase-transferred DMAP stabilized palladium nanoparticles in D_2O.

Figure 10: A comparison between the ^{1}H NMR spectra of the DMAP stabilized palladium nanoparticle dispersion in D_2O obtained (a) one hour and (b) one day after preparation.

Figure 1

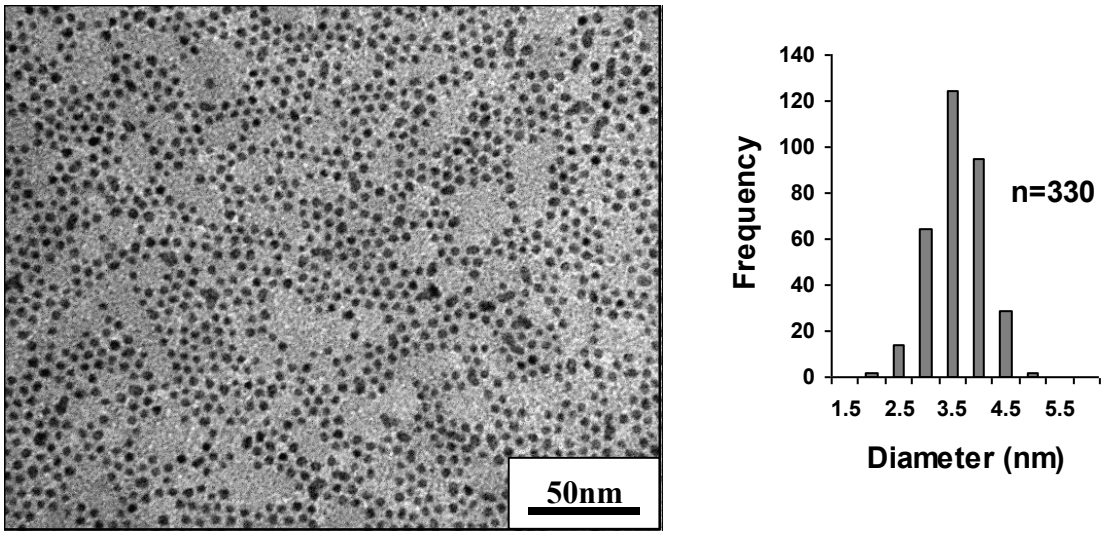

(a) (b)

Figure 1: (a) Transmission electron micrograph of the DMAP stabilized palladium nanoparticles. (b) Histogram of the diameters of 330 nanoparticles with an average diameter of 3.4 nm and a standard deviation of ± 0.5 nm.

Figure 2

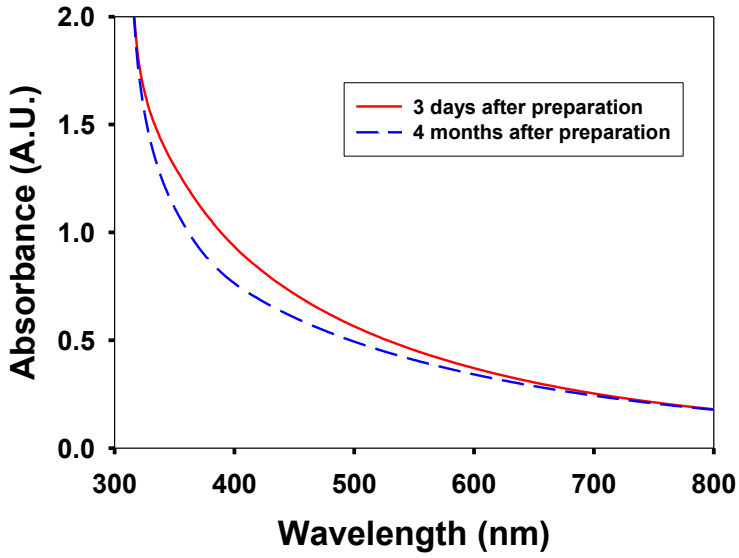

Figure 2: UV-Vis absorption spectra of DMAP stabilized palladium nanoparticles 3 days and 4 months after preparation (The dispersion was diluted 1 in 25 with water).

Figure 3

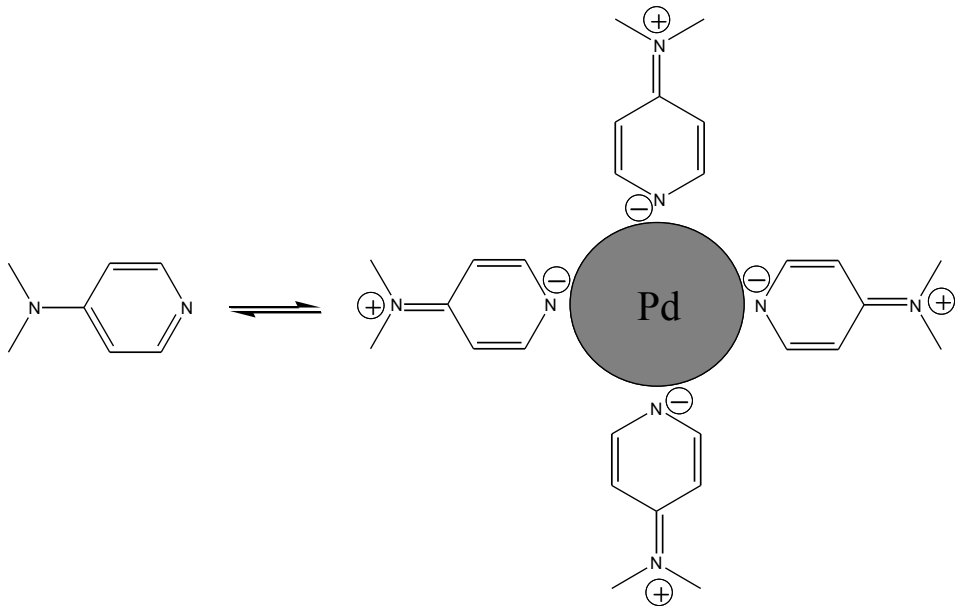

Figure 3: The resonance structures of the DMAP molecule and its proposed interaction with the surface of a palladium nanoparticle.

Figure 4

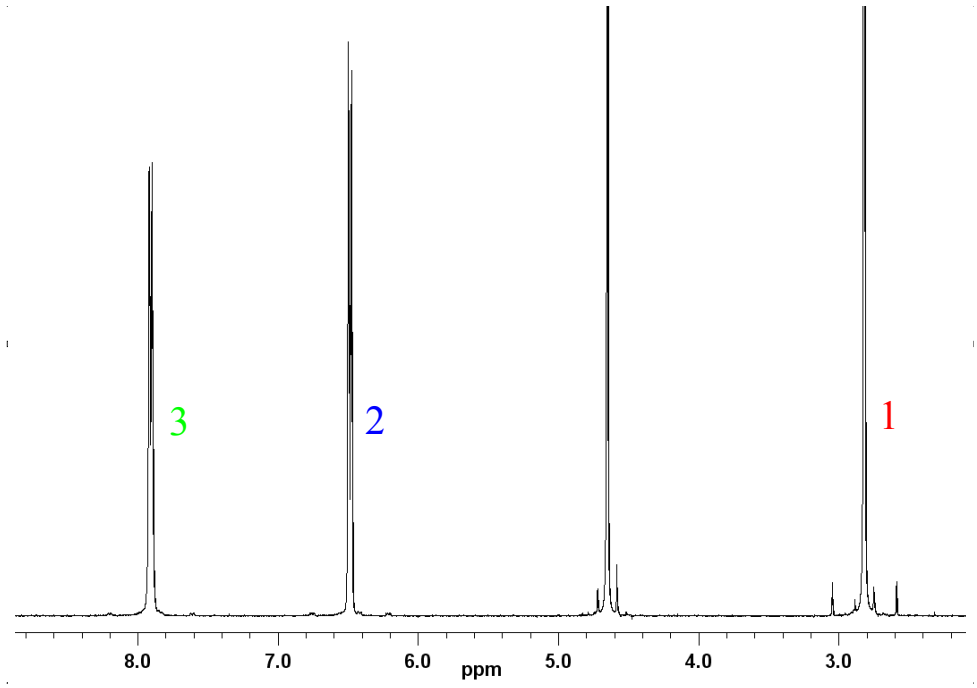

(a)

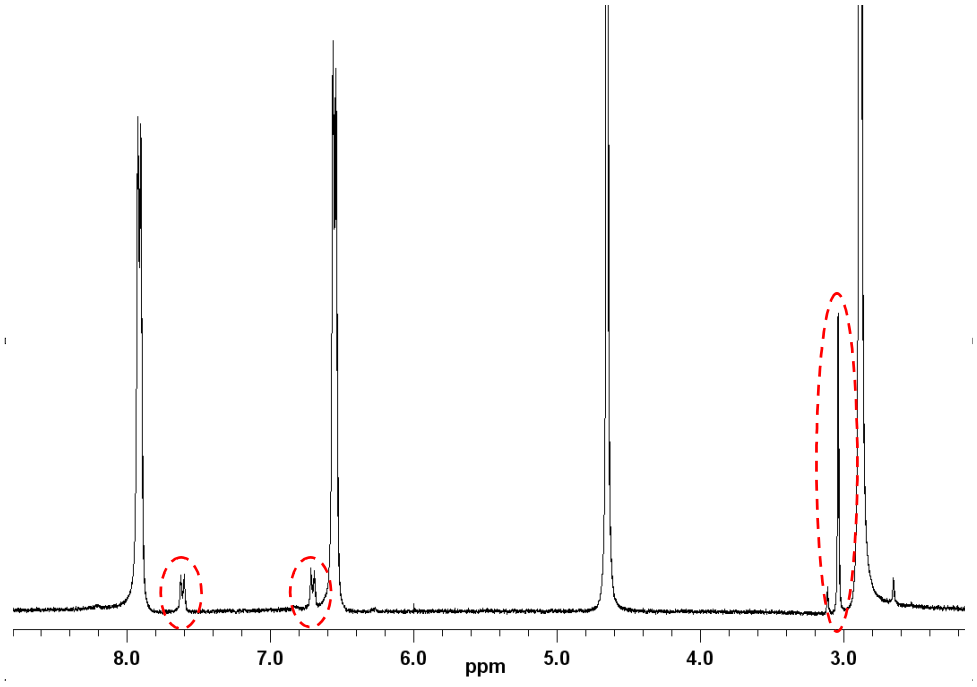

(b)

Figure 4: Representative ^{1}H NMR spectra of (a) DMAP in D_2O and (b) the DMAP stabilized palladium nanoparticle dispersion in D_2O directly following preparation.

Figure 5

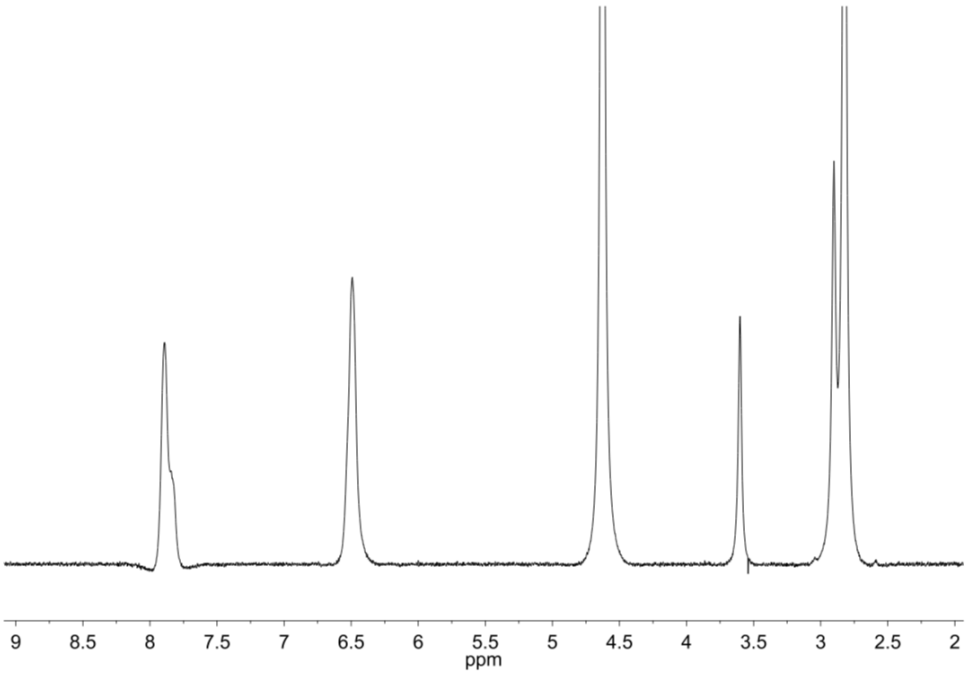

(a)

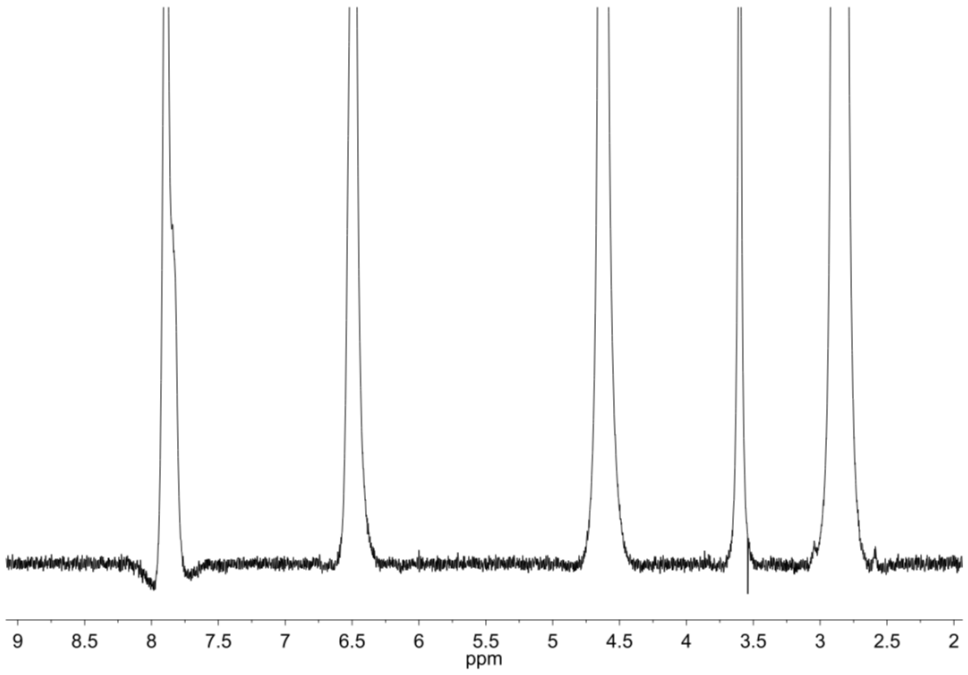

(b)

Figure 5: (a) ^{1}H NMR spectrum of the DMAP stabilized palladium nanoparticle dispersion prepared under an N_2 atmosphere (Resonance at δ 3.61 is attributed to anhydrous 1,4-dioxane, which is used as an internal standard). (b) Magnification of spectrum showing the absence of the other two sets of resonance patterns (a) δ 3.04, δ 6.70 and δ 7.61 and (b) δ 2.77, δ 6.36 and δ 7.76.

Figure 6

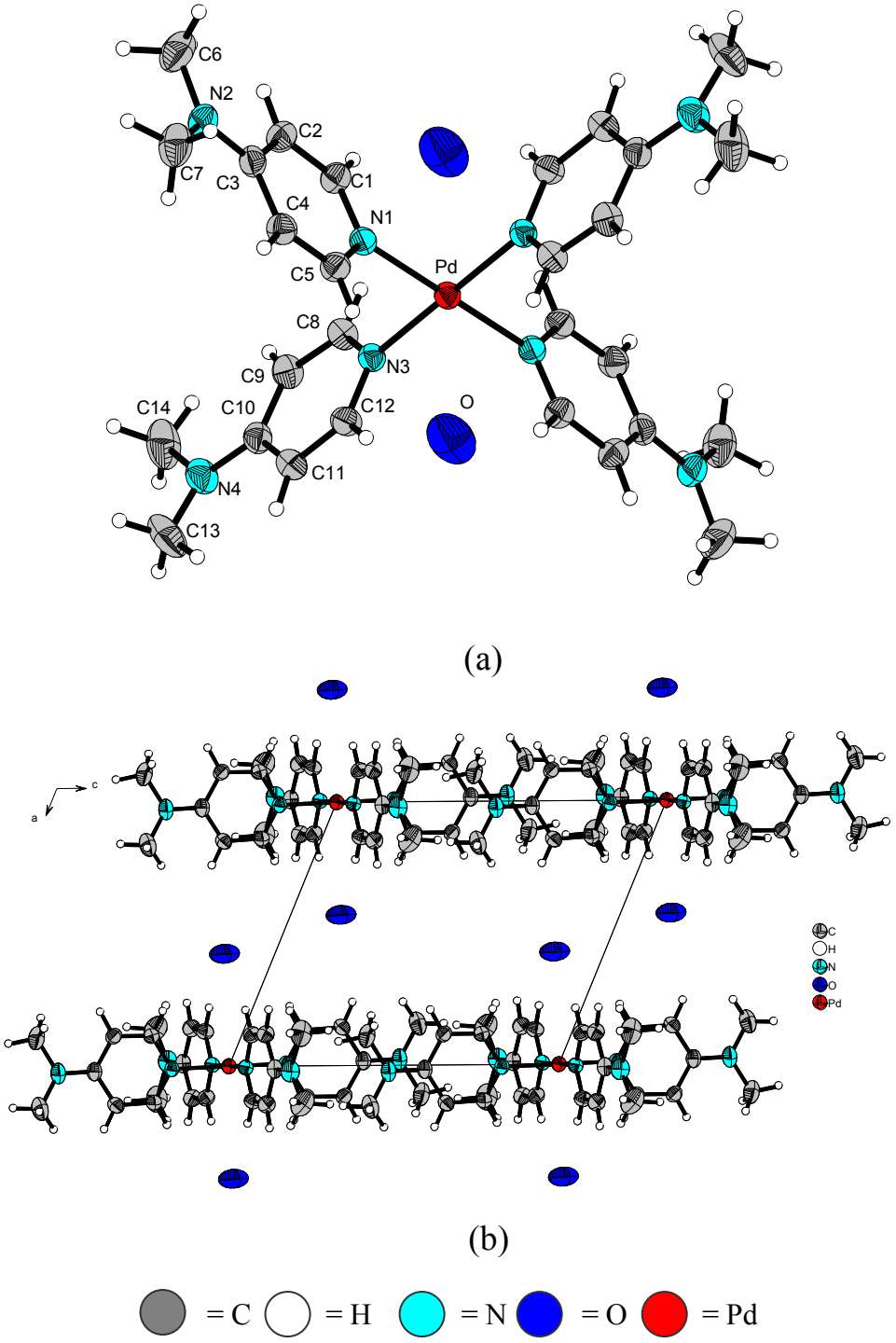

Figure 6: X-Ray crystal structure of the crystals isolated from the DMAP stabilized palladium nanoparticle dispersion: (a) The cationic complex with the two closest counter ions and (b) View along [0 1 0]; the thermal ellipsoids are drawn on the 15% probability level.

Figure 7

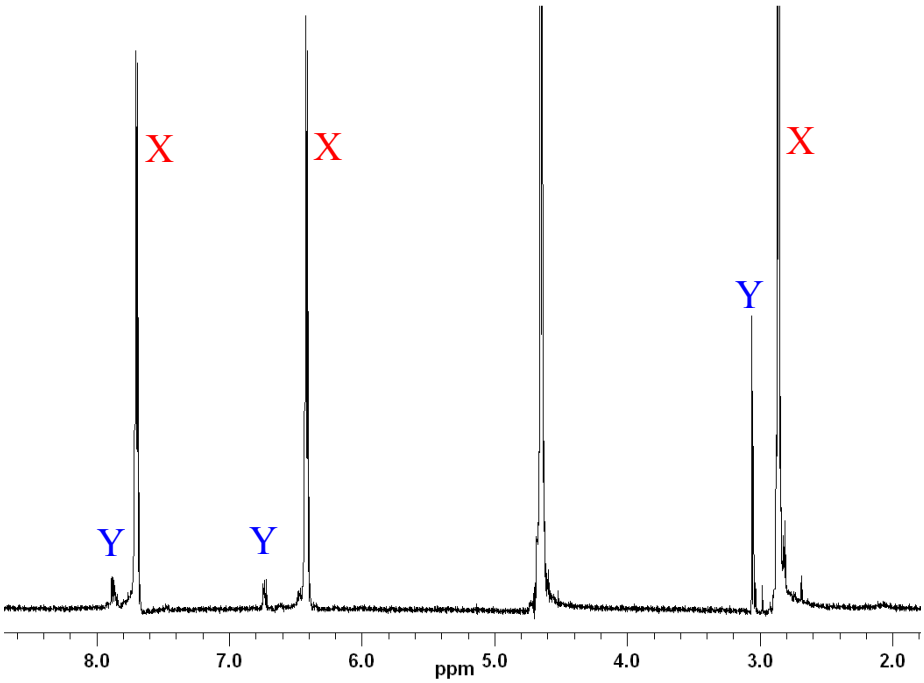

Figure 7: ^{1}H NMR spectrum of the crystals isolated from the DMAP stabilized palladium nanoparticle dispersion.

Figure 8

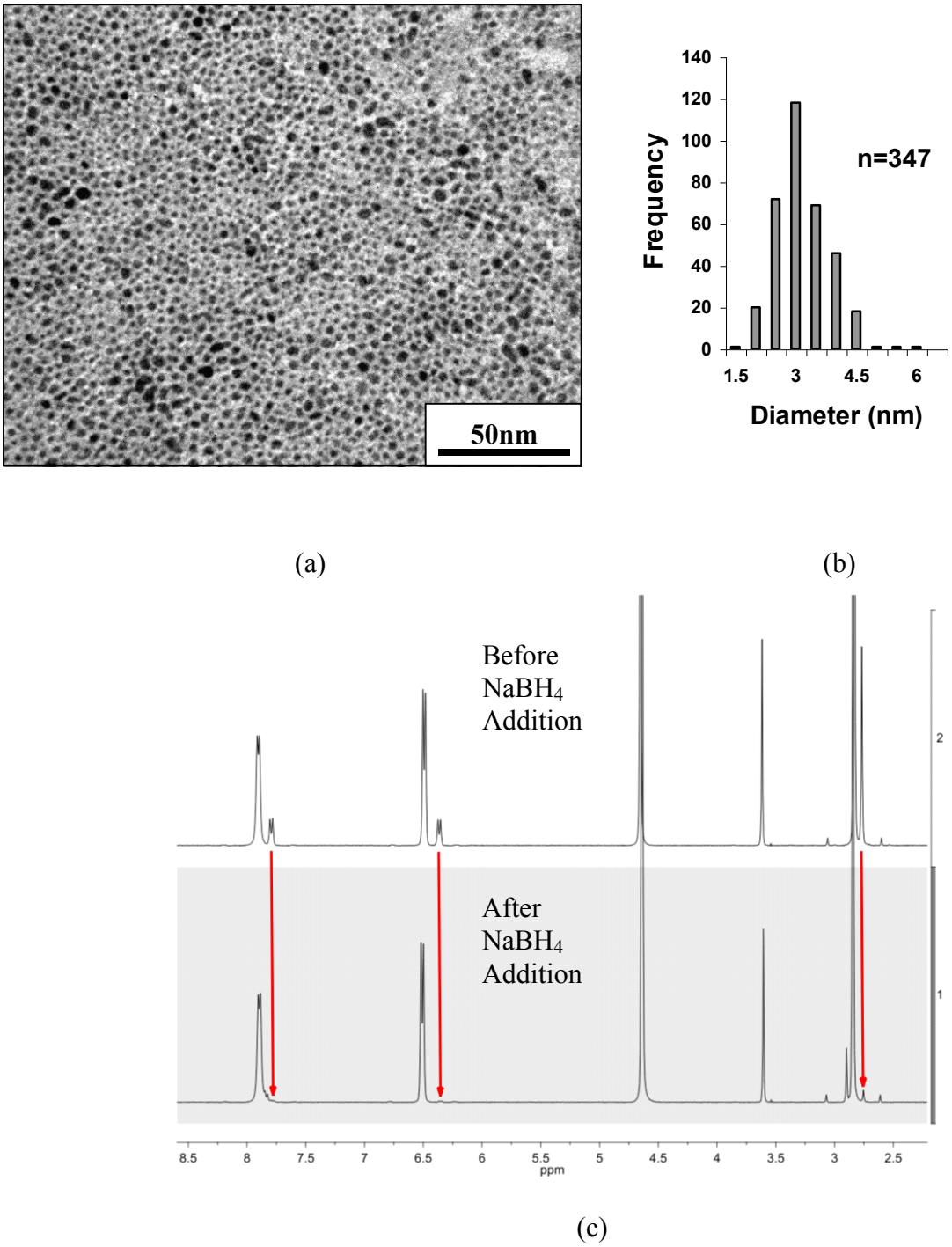

Figure 8: (a) Transmission electron micrograph of the palladium nanoparticles obtained after reduction of a solution of $Pd(DMAP)_4(OH)_2$ complex crystals. (b) Histogram of the diameters of 347 nanoparticles with an average diameter of 2.9 nm and a standard deviation of ± 0.7 nm. (c) ^1H NMR spectrum of $Pd(DMAP)_4(OH)_2$ complex and DMAP before and after addition of $NaBH_4$. The resonances attributed to $Pd(DMAP)_4(OH)_2$ complex are decreased significantly indicating reduction of the complex.

Figure 9

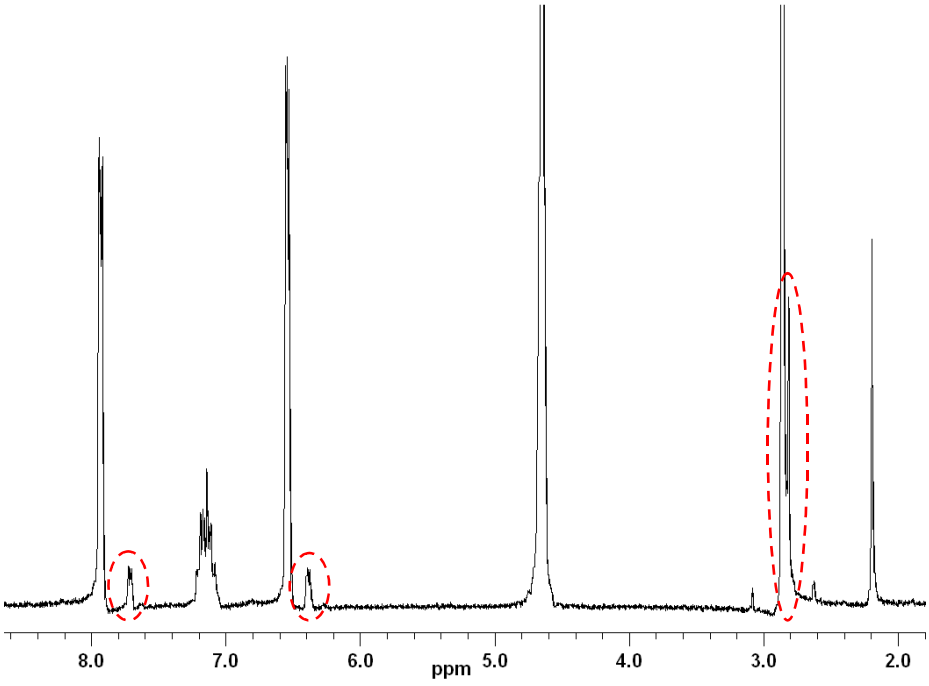

Figure 9: ^{1}H NMR spectrum of phase-transferred DMAP stabilized palladium nanoparticles in D_2O.

Figure 10

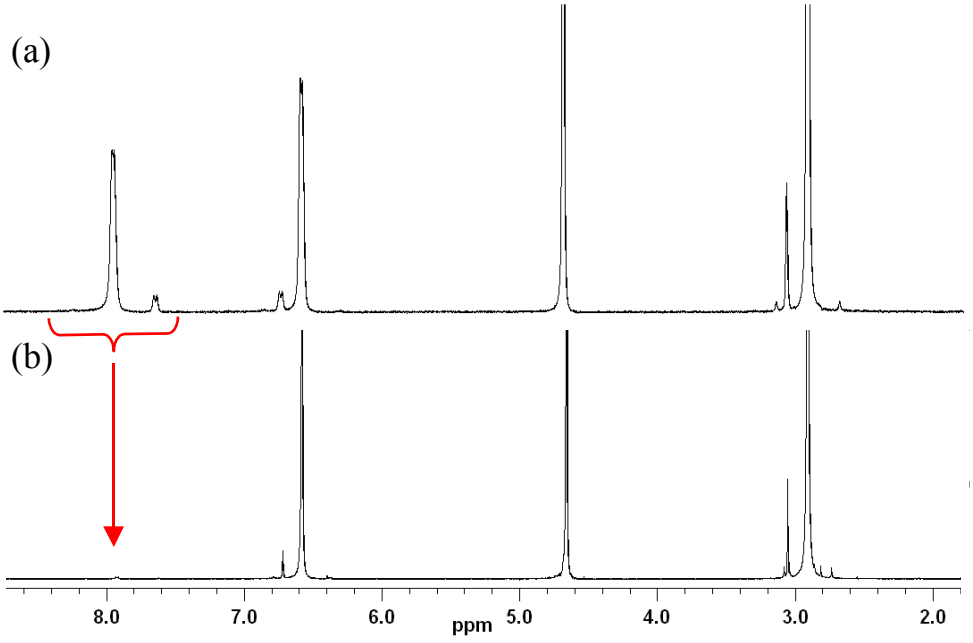

Figure 10: A comparison between the ^{1}H NMR spectra of the DMAP stabilized palladium nanoparticle dispersion in D_2O obtained (a) one hour and (b) one day after preparation.

The Preparation and Characterization of 4-Dimethylaminopyridine (DMAP) Stabilized Palladium Nanoparticles

Keith A. Flanagan, James A. Sullivan and Helge Müeller Bunz.

School of Chemistry and Chemical Biology, UCD, Belfield, Dublin 4, Ireland.

Supporting Information: S1-S13

Figure S1

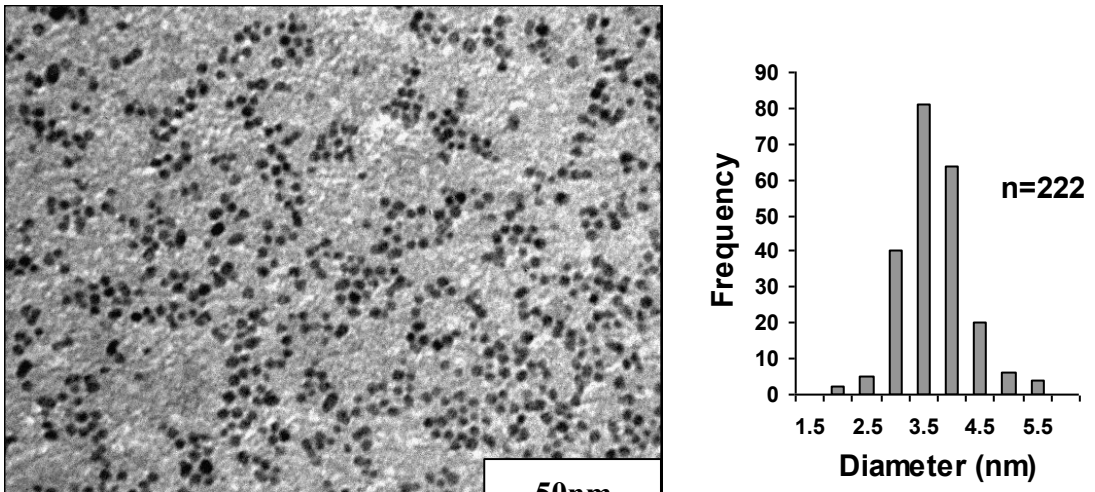

(a) (b)

Figure S1: (a) Transmission electron micrograph of the DMAP stabilized palladium nanoparticles 4 months after preparation. (b) Histogram of the diameters of 222 nanoparticles with an average diameter of 3.4 nm and a standard deviation of ± 0.6 nm.

Figure S2

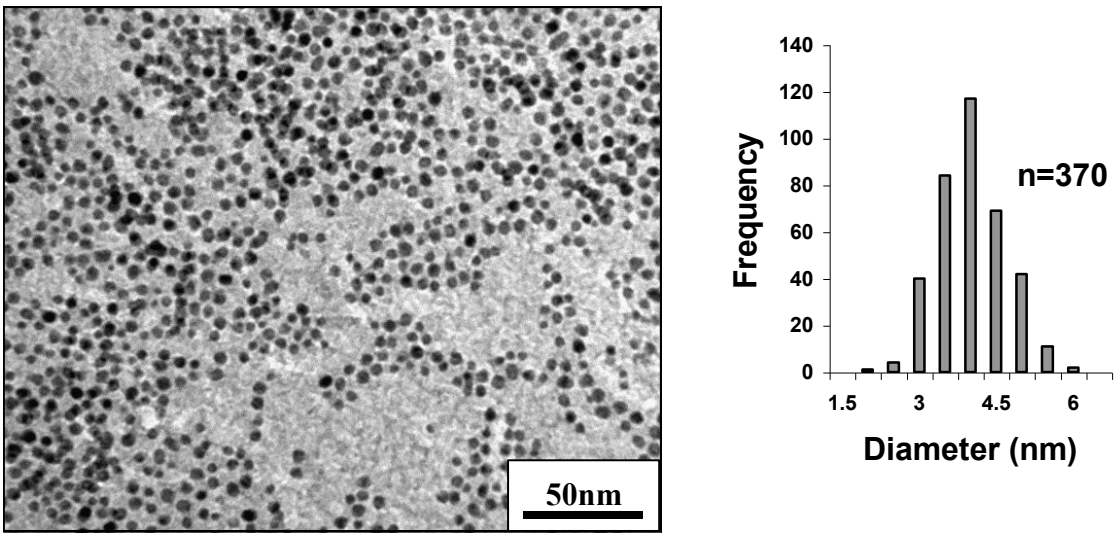

(a) (b)

Figure S2: (a) Transmission electron micrograph of the phase-transferred dodecanethiol stabilized palladium nanoparticles. (b) Histogram of the diameters of 370 nanoparticles with an average diameter of 3.8 nm and a standard deviation of ± 0.7 nm.

Figure S3

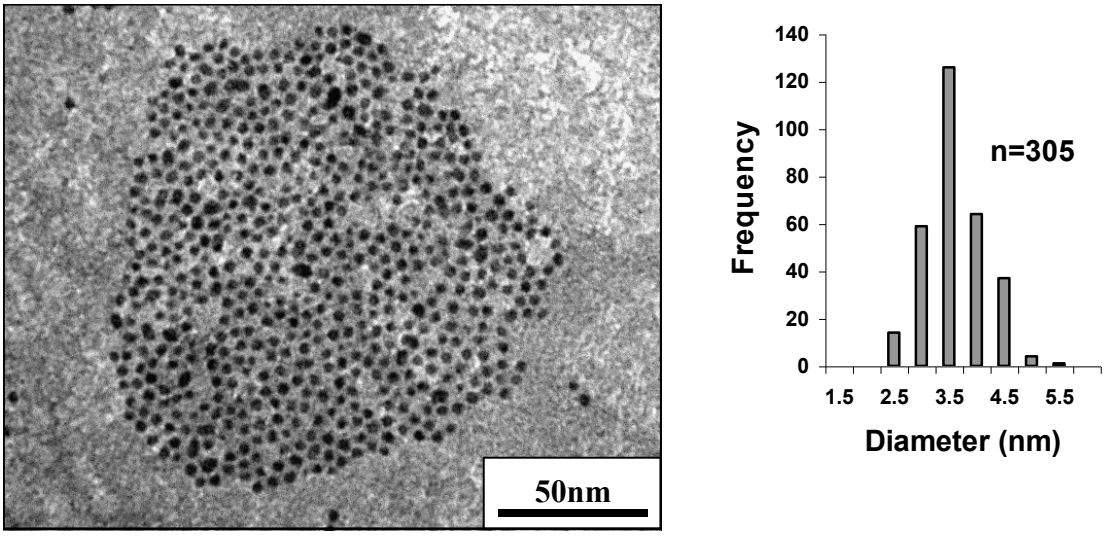

(a) (b)

Figure S3: (a) Transmission electron micrograph of the DMAP stabilized palladium nanoparticles prepared in D_2O. (b) Histogram of the diameters of 305 nanoparticles with an average diameter of 3.4 nm and a standard deviation of ± 0.5 nm. No measurable difference was observed between the nanoparticles obtained from the D_2O preparation and those obtained from the aqueous preparation (3.4 nm ± 0.5 nm) using TEM.

Figure S4

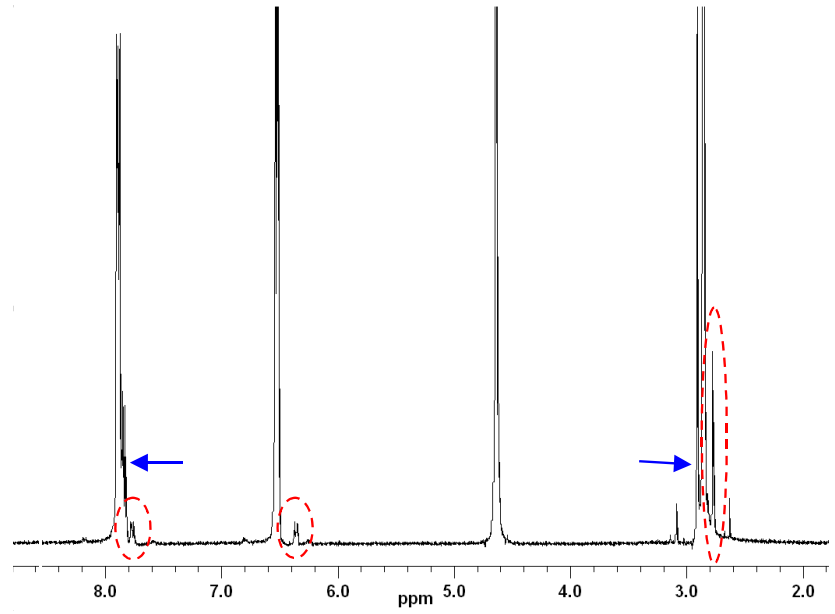

(1)

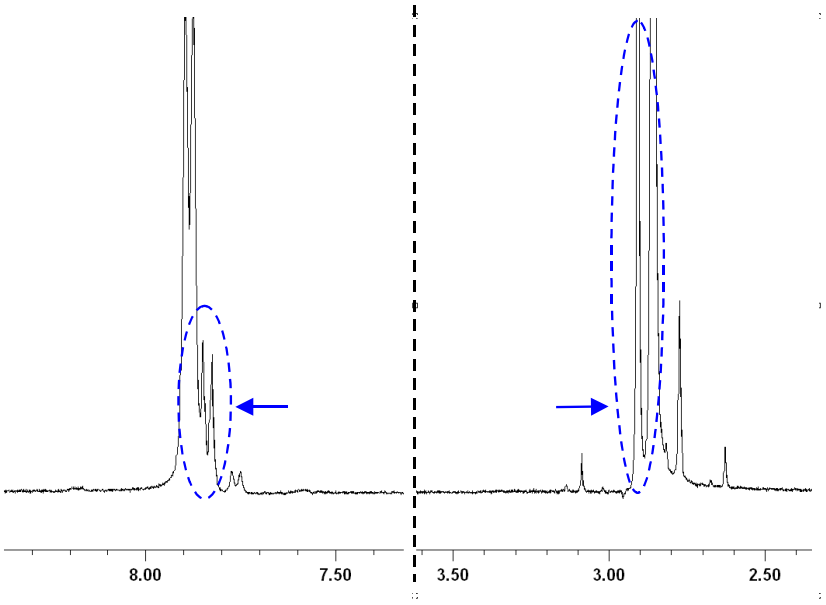

(2)

Figure S4: (1) A further representative ^{1}H NMR spectrum of the DMAP stabilized palladium nanoparticle dispersion in D_2O showing the extra resonance patterns at (b) δ 2.77, δ 6.36 and δ 7.76 and (c) δ 2.91 and δ 7.84. (2) The same ^{1}H NMR spectrum is magnified at selected regions to show resonance pattern (c) in more detail.

Figure S5

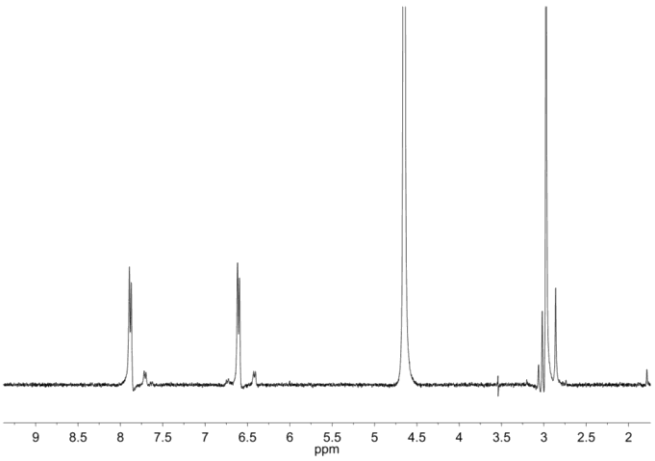

(a)

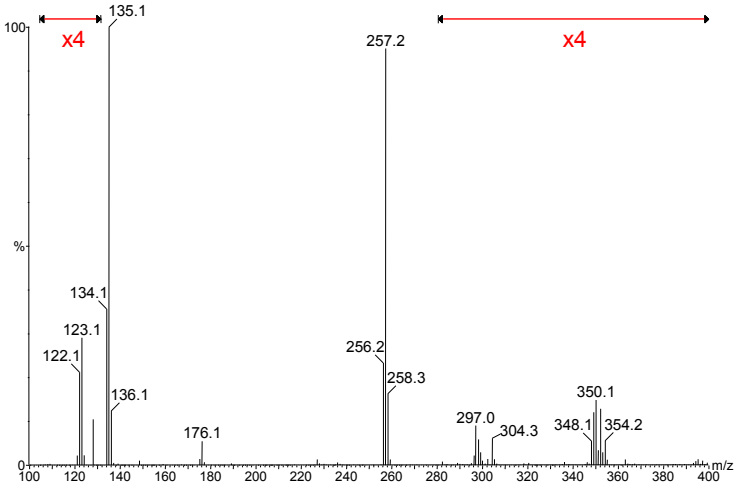

(b)

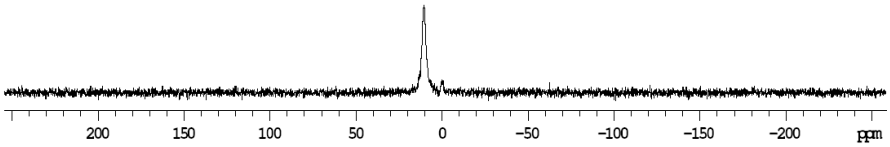

(c)

Figure S5: (a) ^{1}H NMR spectrum of Boron/DMAP complex (Note: Smaller resonances attributed to a trace amount of $Pd(DMAP)_4(OH)_2$ complex are also observed).
(b) Mass spectrum of Boron/DMAP complex showing main isotopic patterns centered at 135.1 and 257.2 which are attributed to B(DMAP) and $B(DMAP)_2$ species respectively [Note: Smaller isotopic patterns (magnified x4) attributed to DMAP (123.1) and a trace amount of $Pd(DMAP)_4(OH)_2$ complex (297.0 and 350.1) are also observed] No other patterns were observed in the spectrum which could be attributed to other DMAP containing complexes.
(c) ^{11}B NMR spectrum of Boron/DMAP complex verifying the presence of boron in the complex.

Figure S6

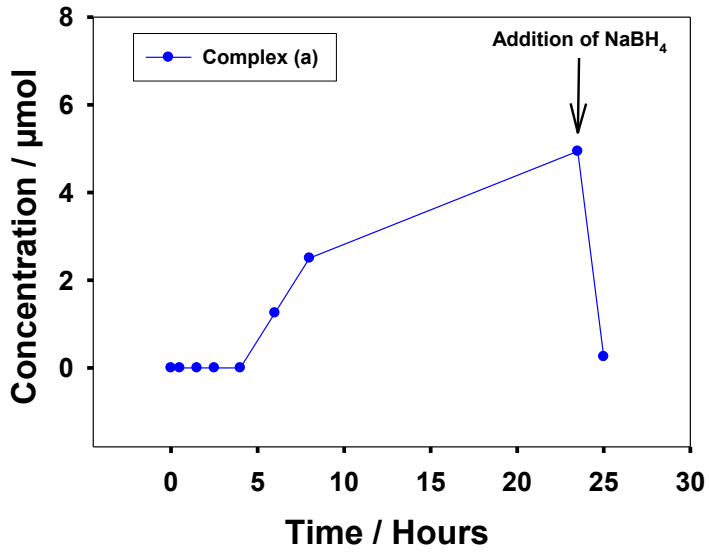

(a)

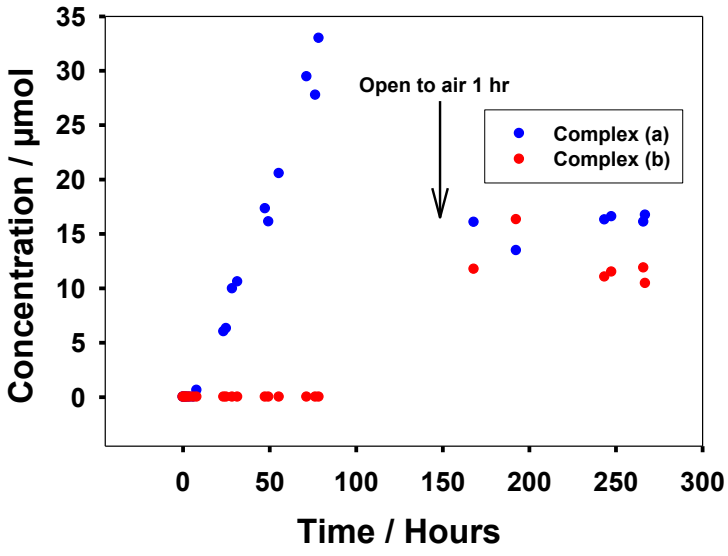

(b)

Figure S6: (a) Plot of the concentration of the first oxidized Pd-DMAP complex in the nanoparticle dispersion [resonance pattern (a) δ 3.04, δ 6.70 and δ 7.61)] as a function of time. $NaBH_4$ in D_2O (1 % w/v, 70 µL) was added to the dispersion at the indicated time. (b) Plot of the concentration of the first and second oxidized Pd-DMAP complexes [resonance pattern (a) δ 3.04, δ 6.70 and δ 7.61) and (b) δ 2.77, δ 6.36 and δ 7.76 respectively]. The nanoparticle dispersion was exposed to air for 1 hour at the indicated time.

Note: Anhydrous 1,4-dioxane (resonance at δ 3.61) was used as an internal standard to monitor the concentration of Pd-DMAP complexes formed over time. The resonance attributed to the methyl group protons attached to the exocyclic nitrogen was used to calculate the concentration.

CIF File S7

```
_audit_creation_method            SHELXL-97
_chemical_name_systematic  ?
_chemical_name_common             ?
_chemical_melting_point           ?
_chemical_formula_moiety
 'C28 H40 N8 Pd, O H, 4.1 (H2 O)'
_chemical_formula_sum
 'C28 H50.2 N8 O6.1 Pd'
_chemical_formula_weight          701.16
loop_
 _atom_type_symbol
 _atom_type_description
 _atom_type_scat_dispersion_real
 _atom_type_scat_dispersion_imag
 _atom_type_scat_source
 'C'  'C'   0.0033   0.0016
 'International Tables Vol C Tables 4.2.6.8 and 6.1.1.4'
 'H'  'H'   0.0000   0.0000
 'International Tables Vol C Tables 4.2.6.8 and 6.1.1.4'
 'N'  'N'   0.0061   0.0033
 'International Tables Vol C Tables 4.2.6.8 and 6.1.1.4'
 'O'  'O'   0.0106   0.0060
 'International Tables Vol C Tables 4.2.6.8 and 6.1.1.4'
 'Pd'  'Pd'  -0.9988   1.0072
 'International Tables Vol C Tables 4.2.6.8 and 6.1.1.4'

_symmetry_cell_setting            Triclinic
_symmetry_space_group_name_H-M    'P -1'

loop_
 _symmetry_equiv_pos_as_xyz
 'x, y, z'
 '-x, -y, -z'

_cell_length_a                    9.7577(17)
_cell_length_b                    11.168(2)
_cell_length_c                    11.261(2)
_cell_angle_alpha                  90.640(3)
_cell_angle_beta                  112.419(3)
_cell_angle_gamma                    95.379(3)
_cell_volume                      1128.0(3)
_cell_formula_units_Z              1
_cell_measurement_temperature     293(2)
_cell_measurement_reflns_used     7832
_cell_measurement_theta_min       2.27
_cell_measurement_theta_max       21.78




_exptl_crystal_description        block
_exptl_crystal_colour             colourless
_exptl_crystal_size_max           0.30
```

```
_exptl_crystal_size_mid          0.20
_exptl_crystal_size_min          0.20
_exptl_crystal_density_meas      ?
_exptl_crystal_density_diffrn    1.032
_exptl_crystal_density_method    'not measured'
_exptl_crystal_F_000             368
_exptl_absorpt_coefficient_mu    0.449
_exptl_absorpt_correction_type   multi-scan
_exptl_absorpt_correction_T_min  0.8091
_exptl_absorpt_correction_T_max  0.9177
_exptl_absorpt_process_details   'SADABS'

_exptl_special_details
;
 ?
;

_diffrn_ambient_temperature      293(2)
_diffrn_radiation_wavelength     0.71073
_diffrn_radiation_type           MoK\a
_diffrn_radiation_source         'fine-focus sealed tube'
_diffrn_radiation_monochromator  graphite
_diffrn_measurement_device_type  'CCD area detector'
_diffrn_measurement_method       'phi and omega scans'
_diffrn_detector_area_resol_mean  ?
_diffrn_standards_number         ?
_diffrn_standards_interval_count  ?
_diffrn_standards_interval_time  ?
_diffrn_standards_decay_%        ?
_diffrn_reflns_number            14806
_diffrn_reflns_av_R_equivalents  0.0223
_diffrn_reflns_av_sigmaI/netI    0.0181
_diffrn_reflns_limit_h_min       -11
_diffrn_reflns_limit_h_max       11
_diffrn_reflns_limit_k_min       -12
_diffrn_reflns_limit_k_max       12
_diffrn_reflns_limit_l_min       -12
_diffrn_reflns_limit_l_max       12
_diffrn_reflns_theta_min         1.83
_diffrn_reflns_theta_max         24.00
_reflns_number_total             3527
_reflns_number_gt                3463
_reflns_threshold_expression     >2sigma(I)




_computing_data_collection       'Bruker SMART'
_computing_cell_refinement       'Bruker SMART'
_computing_data_reduction        'Bruker SAINT'
_computing_structure_solution    'SHELXS-97 (Sheldrick, 1990)'
_computing_structure_refinement  'SHELXL-97 (Sheldrick, 1997)'
_computing_molecular_graphics    'Bruker SHELXTL'
_computing_publication_material  'Bruker SHELXTL'
_refine_special_details
```

Refinement of F^2^ against ALL reflections. The weighted R-factor wR and goodness of fit S are based on F^2^, conventional R-factors R are based on F, with F set to zero for negative F^2^. The threshold expression of F^2^ > 2sigma(F^2^) is used only for calculating R-factors(gt) etc. and is not relevant to the choice of reflections for refinement. R-factors based on F^2^ are statistically about twice as large as those based on F, and R-factors based on ALL data will be even larger.

```
_refine_ls_structure_factor_coef  Fsqd
_refine_ls_matrix_type            full
_refine_ls_weighting_scheme       calc
_refine_ls_weighting_details
 'calc w=1/[\s^2^(Fo^2^)+(0.0938P)^2^+0.0000P] where
P=(Fo^2^+2Fc^2^)/3'
_atom_sites_solution_primary      direct
_atom_sites_solution_secondary    difmap
_atom_sites_solution_hydrogens    geom
_refine_ls_hydrogen_treatment     constr
_refine_ls_extinction_method      none
_refine_ls_extinction_coef        ?
_refine_ls_number_reflns          3527
_refine_ls_number_parameters      202
_refine_ls_number_restraints      0
_refine_ls_R_factor_all           0.0492
_refine_ls_R_factor_gt            0.0485
_refine_ls_wR_factor_ref          0.1263
_refine_ls_wR_factor_gt           0.1252
_refine_ls_goodness_of_fit_ref    1.182
_refine_ls_restrained_S_all       1.182
_refine_ls_shift/su_max           0.001
_refine_ls_shift/su_mean          0.000
loop_
 _atom_site_label
 _atom_site_type_symbol
 _atom_site_fract_x
 _atom_site_fract_y
 _atom_site_fract_z
 _atom_site_U_iso_or_equiv
 _atom_site_adp_type
 _atom_site_occupancy
 _atom_site_symmetry_multiplicity
 _atom_site_calc_flag
 _atom_site_refinement_flags
 _atom_site_disorder_assembly
 _atom_site_disorder_group
Pd Pd 1.0000 1.0000 0.0000 0.07440(18) Uani 1 2 d S . .
N1 N 0.9924(3) 1.0511(2) 0.1697(3) 0.0777(6) Uani 1 1 d . . .
C1 C 0.8635(4) 1.0614(4) 0.1830(4) 0.0894(9) Uani 1 1 d . . .
H1 H 0.7751 1.0397 0.1128 0.107 Uiso 1 1 calc R . .
C2 C 0.8554(5) 1.1018(4) 0.2930(4) 0.0953(10) Uani 1 1 d . . .
```

H2 H 0.7622 1.1061 0.2964 0.114 Uiso 1 1 calc R . .
C3 C 0.9823(5) 1.1370(3) 0.4013(4) 0.0882(9) Uani 1 1 d . . .
N2 N 0.9798(5) 1.1831(4) 0.5097(4) 0.1149(11) Uani 1 1 d . . .
C6 C 0.8399(9) 1.2018(7) 0.5210(7) 0.155(2) Uani 1 1 d . . .
H6A H 0.7745 1.1281 0.4970 0.233 Uiso 1 1 calc R . .
H6B H 0.7941 1.2634 0.4651 0.233 Uiso 1 1 calc R . .
H6C H 0.8586 1.2262 0.6082 0.233 Uiso 1 1 calc R . .
C7 C 1.1144(9) 1.2236(6) 0.6184(5) 0.145(2) Uani 1 1 d . . .
H7A H 1.1877 1.1688 0.6283 0.217 Uiso 1 1 calc R . .
H7B H 1.0932 1.2266 0.6948 0.217 Uiso 1 1 calc R . .
H7C H 1.1521 1.3025 0.6045 0.217 Uiso 1 1 calc R . .
C4 C 1.1180(4) 1.1235(4) 0.3869(4) 0.0937(10) Uani 1 1 d . . .
H4 H 1.2082 1.1432 0.4559 0.112 Uiso 1 1 calc R . .
C5 C 1.1169(4) 1.0819(4) 0.2731(3) 0.0887(9) Uani 1 1 d . . .
H5 H 1.2079 1.0744 0.2665 0.106 Uiso 1 1 calc R . .
N3 N 1.0050(3) 0.8274(3) 0.0519(3) 0.0787(6) Uani 1 1 d . . .
C8 C 0.8816(4) 0.7554(3) 0.0309(4) 0.0909(9) Uani 1 1 d . . .
H8 H 0.7907 0.7841 -0.0153 0.109 Uiso 1 1 calc R . .
C9 C 0.8799(5) 0.6416(4) 0.0730(4) 0.0980(10) Uani 1 1 d . . .
H9 H 0.7893 0.5955 0.0554 0.118 Uiso 1 1 calc R . .
C10 C 1.0128(5) 0.5937(3) 0.1423(4) 0.0921(10) Uani 1 1 d . . .
N4 N 1.0172(6) 0.4850(3) 0.1910(4) 0.1209(13) Uani 1 1 d . . .
C13 C 1.1548(10) 0.4385(6) 0.2676(7) 0.163(3) Uani 1 1 d . . .
H13A H 1.2278 0.4591 0.2312 0.244 Uiso 1 1 calc R . .
H13B H 1.1382 0.3526 0.2687 0.244 Uiso 1 1 calc R . .
H13C H 1.1902 0.4730 0.3539 0.244 Uiso 1 1 calc R . .
C14 C 0.8808(10) 0.4105(5) 0.1765(7) 0.159(3) Uani 1 1 d . . .
H14A H 0.8385 0.4423 0.2328 0.239 Uiso 1 1 calc R . .
H14B H 0.9029 0.3297 0.1980 0.239 Uiso 1 1 calc R . .
H14C H 0.8109 0.4104 0.0891 0.239 Uiso 1 1 calc R . .
C11 C 1.1425(5) 0.6700(4) 0.1598(4) 0.0997(11) Uani 1 1 d . . .
H11 H 1.2353 0.6431 0.2026 0.120 Uiso 1 1 calc R . .
C12 C 1.1343(4) 0.7813(3) 0.1155(4) 0.0921(9) Uani 1 1 d . . .
H12 H 1.2229 0.8291 0.1296 0.110 Uiso 1 1 calc R . .
O1 O 0.5786(6) 0.9522(7) 0.8529(8) 0.256(4) Uani 1 1 d . . .
O2 O 0.5082(19) 0.0706(15) 0.6039(15) 0.256 Uiso 0.564(14) 1 d P . .
O3 O 0.506(3) 0.797(3) 0.059(3) 0.256 Uiso 0.321(15) 1 d P . .

O4 O 0.480(3) 0.3036(19) 0.527(2) 0.256 Uiso 0.436(14) 1 d P . .
O5 O 0.513(3) 0.596(2) 0.123(3) 0.256 Uiso 0.345(14) 1 d P . .
O6 O 0.368(3) 0.513(2) 0.620(2) 0.256 Uiso 0.406(12) 1 d P . .
loop_
 _atom_site_aniso_label
 _atom_site_aniso_U_11
 _atom_site_aniso_U_22
 _atom_site_aniso_U_33
 _atom_site_aniso_U_23
 _atom_site_aniso_U_13
 _atom_site_aniso_U_12
Pd 0.0807(3) 0.0693(2) 0.0739(2) 0.00624(14) 0.03004(16) 0.00900(15)
N1 0.0829(16) 0.0752(15) 0.0757(14) 0.0057(11) 0.0309(12) 0.0096(12)
C1 0.0798(19) 0.098(2) 0.086(2) 0.0024(17) 0.0293(16) 0.0030(16)
C2 0.088(2) 0.104(3) 0.104(3) 0.004(2) 0.048(2) 0.0087(18)

C3 0.111(2) 0.0773(19) 0.085(2) 0.0123(16) 0.0465(19) 0.0125(17)
N2 0.150(3) 0.114(3) 0.093(2) 0.0023(19) 0.060(2) 0.018(2)
C6 0.183(6) 0.181(6) 0.142(5) -0.002(4) 0.102(5) 0.041(5)
C7 0.184(6) 0.152(5) 0.092(3) -0.011(3) 0.047(3) 0.018(4)
C4 0.089(2) 0.102(2) 0.079(2) 0.0026(18) 0.0205(16) 0.0112(18)
C5 0.0759(18) 0.103(2) 0.086(2) 0.0047(18) 0.0279(16) 0.0146(16)
N3 0.0821(16) 0.0748(14) 0.0785(15) 0.0072(12) 0.0298(12) 0.0091(12)
C8 0.088(2) 0.084(2) 0.094(2) 0.0080(17) 0.0279(17) 0.0081(17)
C9 0.105(3) 0.082(2) 0.100(2) 0.0010(18) 0.037(2) -0.0078(19)
C10 0.120(3) 0.074(2) 0.086(2) 0.0041(16) 0.044(2) 0.0143(19)
N4 0.167(4) 0.078(2) 0.122(3) 0.0167(19) 0.059(3) 0.014(2)
C13 0.220(7) 0.110(4) 0.156(5) 0.048(4) 0.059(5) 0.066(5)
C14 0.219(7) 0.094(3) 0.170(6) 0.026(3) 0.085(5) -0.008(4)
C11 0.100(2) 0.094(3) 0.108(3) 0.021(2) 0.038(2) 0.029(2)
C12 0.085(2) 0.088(2) 0.106(2) 0.0124(19) 0.0388(19) 0.0130(17)
O1 0.116(4) 0.287(10) 0.330(10) 0.061(8) 0.047(5) 0.012(4)
_geom_special_details
All esds (except the esd in the dihedral angle between two l.s. planes)
are estimated using the full covariance matrix. The cell esds are taken
into account individually in the estimation of esds in distances, angles
and torsion angles; correlations between esds in cell parameters are only
used when they are defined by crystal symmetry. An approximate (isotropic)
treatment of cell esds is used for estimating esds involving l.s. planes.
_geom_bond_atom_site_label_1
_geom_bond_atom_site_label_2
_geom_bond_distance
_geom_bond_site_symmetry_2
_geom_bond_publ_flag
Pd N1 2.019(3) 2_775 ?
Pd N1 2.019(3) . ?
Pd N3 2.020(3) . ?

Pd N3 2.020(3) 2_775 ?
N1 C5 1.335(5) . ?
N1 C1 1.337(5) . ?
C1 C2 1.346(6) . ?
C1 H1 0.9300 . ?
C2 C3 1.386(6) . ?
C2 H2 0.9300 . ?
C3 N2 1.329(5) . ?
C3 C4 1.415(6) . ?
N2 C7 1.442(8) . ?
N2 C6 1.452(8) . ?
C6 H6A 0.9600 . ?
C6 H6B 0.9600 . ?
C6 H6C 0.9600 . ?
C7 H7A 0.9600 . ?
C7 H7B 0.9600 . ?
C7 H7C 0.9600 . ?
C4 C5 1.355(6) . ?
C4 H4 0.9300 . ?
C5 H5 0.9300 . ?
N3 C8 1.323(5) . ?

```
N3 C12 1.346(5) . ?
C8 C9 1.362(6) . ?
C8 H8 0.9300 . ?
C9 C10 1.394(6) . ?
C9 H9 0.9300 . ?
C10 N4 1.335(5) . ?
C10 C11 1.404(6) . ?
N4 C13 1.440(9) . ?
N4 C14 1.453(9) . ?
C13 H13A 0.9600 . ?
C13 H13B 0.9600 . ?
C13 H13C 0.9600 . ?
C14 H14A 0.9600 . ?
C14 H14B 0.9600 . ?
C14 H14C 0.9600 . ?
C11 C12 1.342(6) . ?
C11 H11 0.9300 . ?
C12 H12 0.9300 . ?
loop_
 _geom_angle_atom_site_label_1
 _geom_angle_atom_site_label_2
 _geom_angle_atom_site_label_3
 _geom_angle
 _geom_angle_site_symmetry_1
 _geom_angle_site_symmetry_3
 _geom_angle_publ_flag
```

```
N1 Pd N1 179.999(1) 2_775 . ?
N1 Pd N3 90.25(11) 2_775 . ?
N1 Pd N3 89.75(11) . . ?
N1 Pd N3 89.76(11) 2_775 2_775 ?
N1 Pd N3 90.24(11) . 2_775 ?
N3 Pd N3 180.00(17) . 2_775 ?
C5 N1 C1 116.6(3) . . ?
C5 N1 Pd 121.3(2) . . ?
C1 N1 Pd 122.0(2) . . ?
N1 C1 C2 123.3(3) . . ?
N1 C1 H1 118.4 . . ?
C2 C1 H1 118.4 . . ?
C1 C2 C3 121.7(3) . . ?
C1 C2 H2 119.2 . . ?
C3 C2 H2 119.2 . . ?
N2 C3 C2 123.8(4) . . ?
N2 C3 C4 121.7(4) . . ?
C2 C3 C4 114.5(3) . . ?
C3 N2 C7 122.1(5) . . ?
C3 N2 C6 121.1(5) . . ?
C7 N2 C6 116.7(5) . . ?
N2 C6 H6A 109.5 . . ?
N2 C6 H6B 109.5 . . ?
H6A C6 H6B 109.5 . . ?
```

N2 C6 H6C 109.5 . . ?
H6A C6 H6C 109.5 . . ?
H6B C6 H6C 109.5 . . ?
N2 C7 H7A 109.5 . . ?
N2 C7 H7B 109.5 . . ?
H7A C7 H7B 109.5 . . ?
N2 C7 H7C 109.5 . . ?
H7A C7 H7C 109.5 . . ?
H7B C7 H7C 109.5 . . ?
C5 C4 C3 120.2(3) . . ?
C5 C4 H4 119.9 . . ?
C3 C4 H4 119.9 . . ?
N1 C5 C4 123.6(3) . . ?
N1 C5 H5 118.2 . . ?
C4 C5 H5 118.2 . . ?
C8 N3 C12 116.3(3) . . ?
C8 N3 Pd 121.9(2) . . ?
C12 N3 Pd 121.7(2) . . ?
N3 C8 C9 123.8(4) . . ?
N3 C8 H8 118.1 . . ?
C9 C8 H8 118.1 . . ?
C8 C9 C10 120.6(4) . . ?

C8 C9 H9 119.7 . . ?
C10 C9 H9 119.7 . . ?
N4 C10 C9 123.0(4) . . ?
N4 C10 C11 122.3(4) . . ?
C9 C10 C11 114.7(3) . . ?
C10 N4 C13 122.6(5) . . ?
C10 N4 C14 121.0(5) . . ?
C13 N4 C14 116.3(5) . . ?
N4 C13 H13A 109.5 . . ?
N4 C13 H13B 109.5 . . ?
H13A C13 H13B 109.5 . . ?
N4 C13 H13C 109.5 . . ?
H13A C13 H13C 109.5 . . ?
H13B C13 H13C 109.5 . . ?
N4 C14 H14A 109.5 . . ?
N4 C14 H14B 109.5 . . ?
H14A C14 H14B 109.5 . . ?
N4 C14 H14C 109.5 . . ?
H14A C14 H14C 109.5 . . ?
H14B C14 H14C 109.5 . . ?
C12 C11 C10 120.9(4) . . ?
C12 C11 H11 119.5 . . ?
C10 C11 H11 119.5 . . ?
C11 C12 N3 123.6(4) . . ?
C11 C12 H12 118.2 . . ?
N3 C12 H12 118.2 . . ?
loop_
 _geom_torsion_atom_site_label_1
 _geom_torsion_atom_site_label_2
 _geom_torsion_atom_site_label_3

```
 _geom_torsion_atom_site_label_4
 _geom_torsion
 _geom_torsion_site_symmetry_1
 _geom_torsion_site_symmetry_2
 _geom_torsion_site_symmetry_3
 _geom_torsion_site_symmetry_4
 _geom_torsion_publ_flag
N1 Pd N1 C5 10(38) 2_775 . . . ?
N3 Pd N1 C5 89.6(3) . . . . ?
N3 Pd N1 C5 -90.4(3) 2_775 . . . ?
N1 Pd N1 C1 -173(38) 2_775 . . . ?
N3 Pd N1 C1 -93.8(3) . . . . ?
N3 Pd N1 C1 86.2(3) 2_775 . . . ?
C5 N1 C1 C2 0.7(6) . . . . ?
Pd N1 C1 C2 -176.1(3) . . . . ?
N1 C1 C2 C3 0.7(6) . . . . ?
C1 C2 C3 N2 176.4(4) . . . . ?
C1 C2 C3 C4 -1.8(6) . . . . ?


C2 C3 N2 C7 -177.2(5) . . . . ?
C4 C3 N2 C7 0.9(7) . . . . ?
C2 C3 N2 C6 -1.0(7) . . . . ?
C4 C3 N2 C6 177.0(5) . . . . ?
N2 C3 C4 C5 -176.6(4) . . . . ?
C2 C3 C4 C5 1.6(6) . . . . ?
C1 N1 C5 C4 -0.8(6) . . . . ?
Pd N1 C5 C4 176.0(3) . . . . ?
C3 C4 C5 N1 -0.3(6) . . . . ?
N1 Pd N3 C8 -93.0(3) 2_775 . . . ?
N1 Pd N3 C8 87.0(3) . . . . ?
N3 Pd N3 C8 90(29) 2_775 . . . ?
N1 Pd N3 C12 90.3(3) 2_775 . . . ?
N1 Pd N3 C12 -89.7(3) . . . . ?
N3 Pd N3 C12 -86(29) 2_775 . . . ?
C12 N3 C8 C9 2.1(6) . . . . ?
Pd N3 C8 C9 -174.8(3) . . . . ?
N3 C8 C9 C10 -0.3(7) . . . . ?
C8 C9 C10 N4 176.6(4) . . . . ?
C8 C9 C10 C11 -1.8(6) . . . . ?
C9 C10 N4 C13 -177.0(5) . . . . ?
C11 C10 N4 C13 1.4(7) . . . . ?
C9 C10 N4 C14 -1.4(7) . . . . ?
C11 C10 N4 C14 177.0(5) . . . . ?
N4 C10 C11 C12 -176.4(4) . . . . ?
C9 C10 C11 C12 2.1(6) . . . . ?
C10 C11 C12 N3 -0.4(7) . . . . ?
C8 N3 C12 C11 -1.7(6) . . . . ?
Pd N3 C12 C11 175.1(3) . . . . ?
_diffrn_measured_fraction_theta_max    0.997
_diffrn_reflns_theta_full              24.00
_diffrn_measured_fraction_theta_full   0.997
_refine_diff_density_max    0.671
_refine_diff_density_min   -0.366
_refine_diff_density_rms    0.092
```

Figure S8

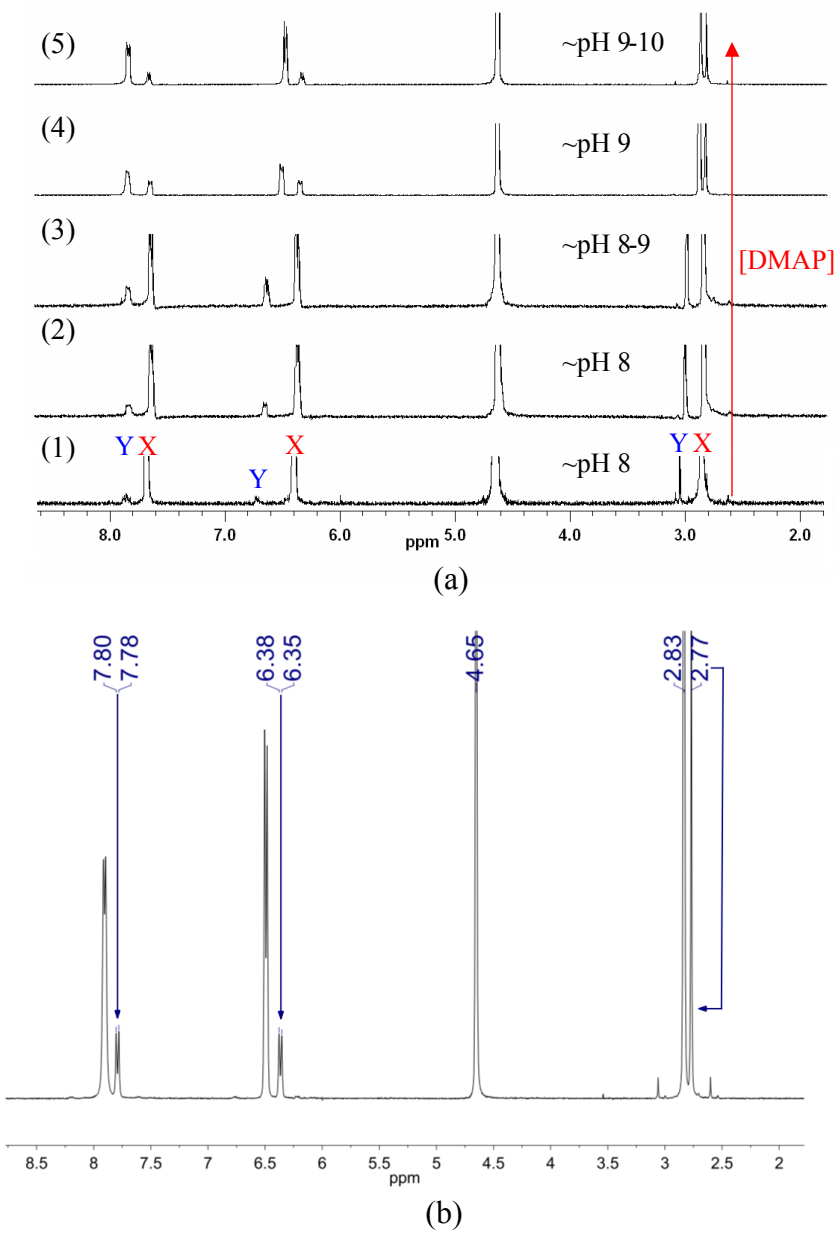

Figure S8: (a) ^{1}H NMR spectra of isolated $Pd(DMAP)_4(OH)_2$ complex crystals with an increasing amount of added DMAP (Concentration of DMAP increases from spectra 1 to 5). This verifies that the resonances in set (Y) are due to trace amounts of free DMAP retained on the crystals following their isolation from the nanoparticle dispersion. (b) ^{1}H NMR spectrum showing the positions of the DMAP and complex resonances when the pH is adjusted through the addition of DMAP to the pH of the nanoparticle dispersion. At this pH the complex shows resonances at (δ 2.77, δ 6.37 and δ 7.79) which almost exactly match those of resonance pattern (b) (δ 2.77, δ 6.36 and δ 7.76) seen in the ^{1}H NMR spectrum of the dispersion.

Figure S9

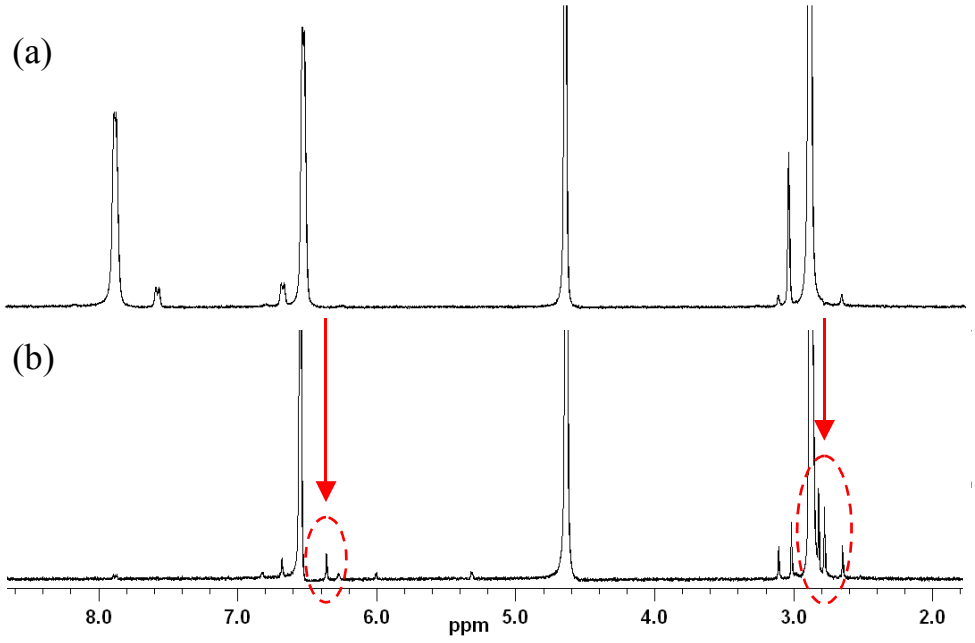

Figure S9: A comparison between the ^{1}H NMR spectra of the DMAP stabilized palladium nanoparticle dispersion in D_2O obtained (a) one hour and (b) five days after preparation. This demonstrates that the resonances observed for palladium/DMAP complexes could interchange from one pattern to another over time under atmospheric conditions.

Figure S10

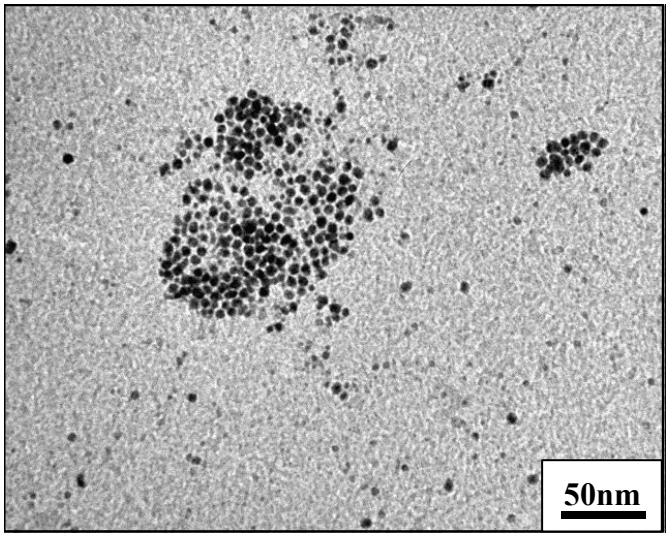

Figure S10: Transmission electron micrograph of DMAP stabilized palladium nanoparticles prepared using the phase-transfer procedure reported by Gittins *et al.*[16]

Figure S11

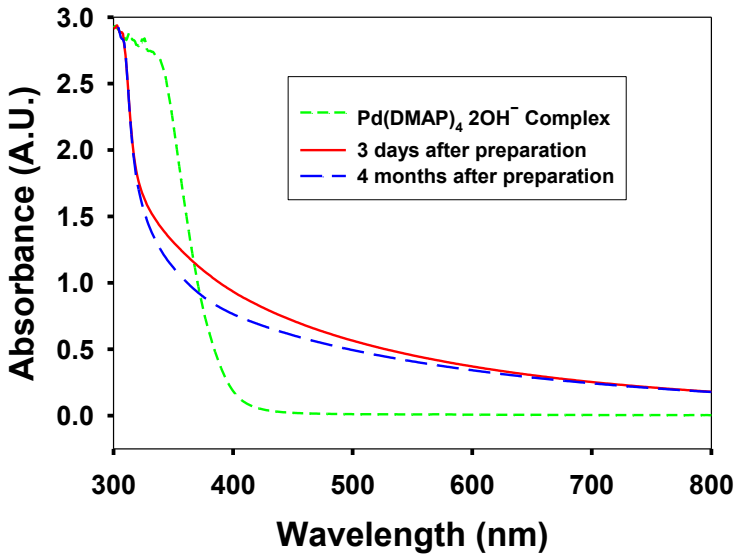

Figure S11: UV-Vis absorption spectra of DMAP stabilized palladium nanoparticles 3 days and 4 months after preparation (The dispersion was diluted 1 in 25 with water) along with a spectrum of a solution of $Pd(DMAP)_4(OH)_2$ crystals which have been isolated from the nanoparticle dispersion. No obvious absorption bands that are attributable to such palladium/DMAP complexes are observed in the 3 day old or even the 4 month old nanoparticle dispersions.

Figure S12

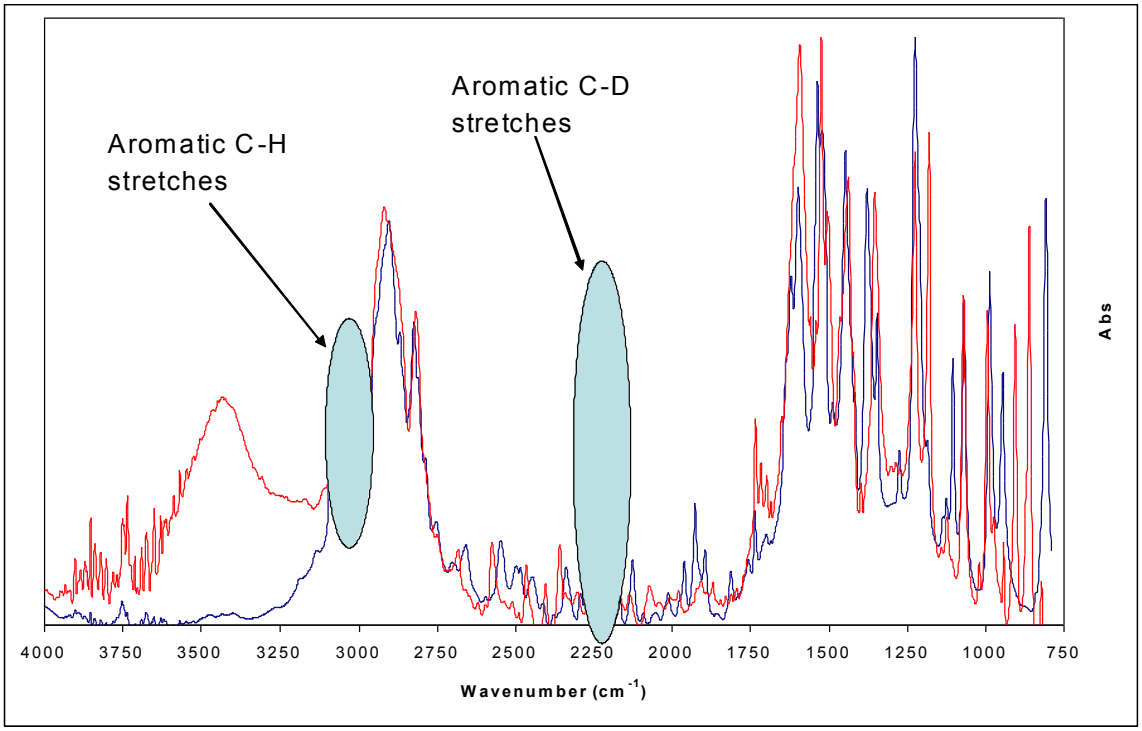

Figure S12: Normalized FTIR spectra of 99% pure DMAP (blue) and DMAP removed from a palladium nanoparticle dispersion prepared in D_2O after 1 day (red). Peaks due to the aromatic C-H and C-D stretches are highlighted. The affects of selective hydrogen/deuterium (H/D) exchange on the carbon atoms α to the endocyclic nitrogen atom on the DMAP removed from the palladium nanoparticle dispersion are observed.

Figure S13

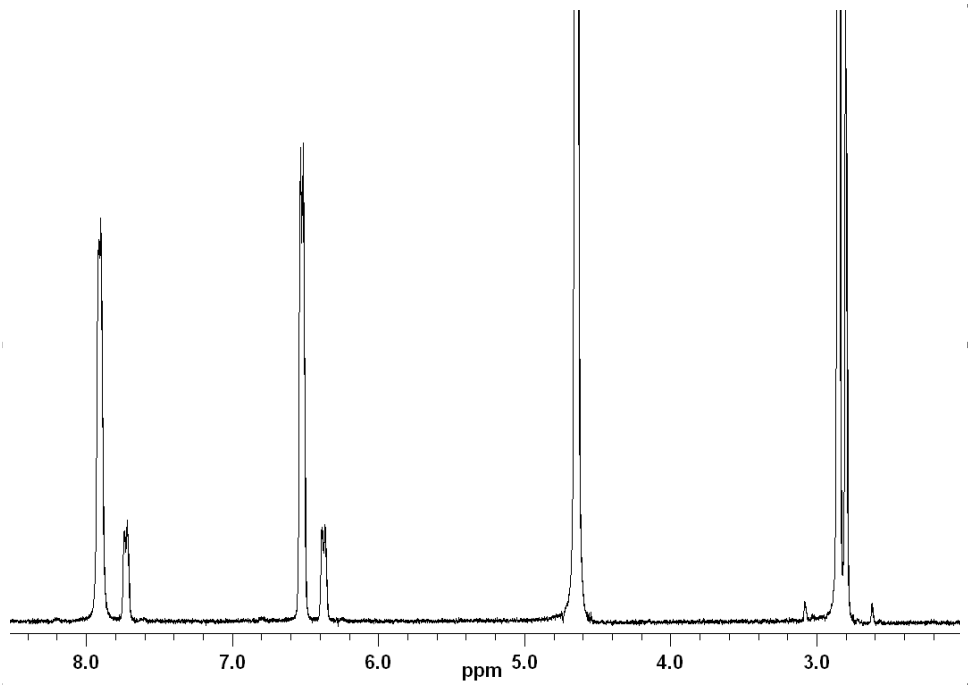

Figure S13: ^{1}H NMR spectrum of $Pd(DMAP)_4(OH)_2$ complex with additional DMAP showing no selective hydrogen/deuterium (H/D) exchange on the carbon atoms α to the endocyclic nitrogen atom on DMAP in the absence of nanoparticles.